Armed Services Technical Information Agency

AD

44486

UNCLASSIFIED

WASHINGTON UNIVERSITY

Departments of Physics and Chemistry

St. Louis 5, Missouri

TECHNICAL REPORT No.

14. Spin Relaxation in Free Radical Solutions Exhibiting Hyperfine Structure, - J. P. Lloyd and G. E. Pake

15. Symmetry Classification of the Energy Levels of Some Triarylmethyl Free Radicals and Their Cations - T. L. Chu and S. I. Weissman

16. Paramagnetic Resonance Spectra of Wurster's Free Radical Ions - S. I. Weissman

17. Electron Transfer Between Naphthalene Negative Ion and Naphthalene - R. L. Ward and S. I. Weissman

18. A Study of Manganous Complexes by Paramagnetic Resonance Absorption - M. Cohn and J. Townsend

October 1, 1954

CONTRACT N6 ONR-202, TASK ORDER 05
(Paramagnetic Resonance)

with

OFFICE OF NAVAL RESEARCH
U. S. NAVY DEPARTMENT
RDB No. NR 310-802

Spin Relaxation in Free Radical Solutions Exhibiting Hyperfine Structure*

J. P. LLOYD† AND G. E. PAKE

Department of Physics, Washington University, Saint Louis, Missouri

(Received January 15, 1954)

Experimental studies of spin-lattice relaxation in aqueous solutions of the free radical peroxylamine disulfonate ion, $ON(SO_3)_2^{--}$, have been made in fields near 30 oersteds. The continuous wave saturation technique was used to study the transition $F=\frac{3}{2}$, $m_F=-\frac{3}{2} \to F=\frac{3}{2}$, $m_F=-\frac{1}{2}$, for which the frequency was 60 Mc sec^{-1}. Because the hyperfine interaction of the unpaired electron with the N^{14} nucleus leads to six unequally spaced energy levels, a unique relaxation time cannot be defined. A general treatment of the saturation method leads to definition of the *relaxation probability*, which reduces for a system with two energy levels to the reciprocal of twice the relaxation time. The experimentally measured relaxation probability is found to be concentration independent below 0.005 molar in $ON(SO_3)_2^{--}$, approaching an asymptotic value of 2×10^6 sec^{-1}. Experiment and theory both rule out as the source for this relaxation probability the interaction of the electron moment with the nuclear moments

of the H_2O solvent molecules, and theory also rules out the effect of the N^{14} electric quadrupole coupling to solvent motions; the latter can, in principle, effect electron relaxation because of the hyperfine coupling between the N^{14} nuclear spin and the electron spin. Estimates are made of the role played by spin-orbit coupling, and it appears probable that the observed relaxation involves this interaction. An interesting by-product of the analysis of the relaxation probability is the result that second order statistical processes, by which an electron spin is first carried with energy conservation to an excited Stark level before reaching the ground Stark level of opposite spin, may account for the observed relaxation. This process is somewhat similar to the Raman processes invoked by Van Vleck to explain relaxation in the alums, except that in Van Vleck's theory the intermediate excited Stark level is only virtually occupied, without energy conservation.

1. INTRODUCTION

THE paramagnetic resonance of the peroxylamine disulfonate ion, $ON(SO_3)_2^{--}$, even in crystals of the potassium salt, is not characterized by the pronounced exchange narrowing frequently observed for free radical molecules. It is perhaps attributable to this weakness of the exchange interaction that one can observe a well-resolved hyperfine splitting from the N^{14} nucleus in liquid solutions containing this ion in concentrations even larger than 0.1 molar.[1] There is, therefore, a range of concentrations over which magnetic dipole transitions of the coupled system, electronic moment plus nuclear moment, can be observed in fields near 10 gauss with adequate signal-to-noise. Measurements by Townsend[2] have shown that, in fields up to 50 gauss and at frequencies between 9 and 120 Mc/sec, the Breit-Rabi energy levels for a system with $I=1$, $J=\frac{1}{2}$ apply to the peroxylamine disulfonate ion in solution.

The present work concerns itself with the mechanism which maintains the population differential between a particular pair of levels participating in resonance absorption. This mechanism will also be shown in the system at hand to dominate in producing the observed line width. The mechanisms of interest in determining measured widths of paramagnetic resonances are, in general, the spin-spin and spin-lattice interactions, which may occasionally be markedly obscured by instrumental effects. The advantages of working in low fields (~30 gauss) are twofold. First, the individual hyperfine components become only a fraction of a gauss wide at concentrations below about 10^{-2} molar. In the

magnetic fields of several thousand gauss which correspond to microwave frequencies, care must be exercised to assure that field inhomogeneities over the sample do not mask the true line width. However, if Helmholtz coils or a solenoid are used in producing the 30-gauss field, no effort at all is required to keep inhomogeneities below 10^{-2} gauss over a sample of several cubic centimeters volume. A second advantage is more compelling. To separate non-negligible spin-spin processes, if any, from the spin-lattice interactions limiting the lifetime of a spin state, one needs to know the spin-lattice relaxation time. While this can be measured with difficulty at microwave frequencies,[3,4] microwave generators with adequate power are not presently available in this laboratory, and the techniques, in any event, are not as easily applied as those using lumped parameter circuits.

The Hamiltonian function describing the interaction leading to the hyperfine structure is[5]

$$\mathcal{H} = g_J \mu_0 H_0 J_z + a \mathbf{I} \cdot \mathbf{J} - g_I \mu_0 H_0 I_z \qquad (1)$$

where g_J is the spectroscopic splitting factor for the free radical; for a free electron $g_J = g_e = 2.0023$. The magnitude of the Bohr magneton is μ_0, and the antiparallellity of J and the magnetic moment of the electron is explicitly taken into account by the positive sign preceding the first term of (1). H_0 is the applied external field, and a is the hyperfine coupling constant. Since we take g_I as the nuclear g factor referred to the (positive) Bohr magneton μ_0, it is the conventional nuclear g divided by $M/m = 1836$.

The Breit-Rabi energy levels[5] given by the Hamil-

* Assisted by the joint program of the U. S. Office of Naval Research and the U. S. Atomic Energy Commission.
† Now at Shell Oil Company, Houston, Texas.
[1] Pake, Townsend, and Weissman, Phys. Rev. 85, 682 (1952).
[2] Townsend, Weissman, and Pake, Phys. Rev. 89, 606 (1953).

[3] C. P. Slichter, thesis, Harvard University (unpublished); also Phys. Rev. 76, 465 (1949).
[4] E. E. Schneider and T. S. England, Physica 17, 221 (1951).
[5] G. Breit and I. I. Rabi, Phys. Rev. 38, 2082 (1931). See also J. E. Nafe and E. D. Nelson, Phys. Rev. 73, 718 (1948).
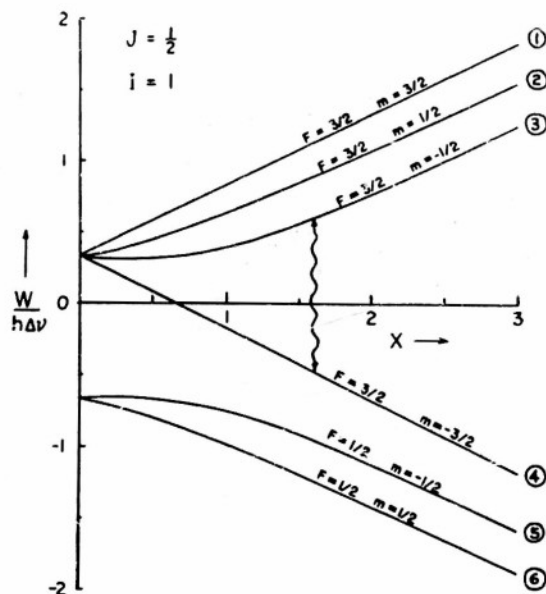
FIG. 1. Breit-Rabi levels for the $ON(SO_3)_2^{--}$ ions. The transition marked is that for which rf saturation measurements were made as a function of concentration in aqueous solution.

tonian (1) for $I=1$, $J=\frac{1}{2}$ are displayed in Fig. 1. The particular transition studied in the present work is that between the levels $F=\frac{3}{2}$, $m_F=-\frac{1}{2}$ and $F=\frac{3}{2}$, $m_F=-\frac{3}{2}$. This transition has a frequency which increases monotonically from zero. However, the ratio of frequency to field is not effectively constant until large enough fields are attained to decouple J from I. In order to treat the spin interaction processes later on, we reproduce here the wave functions and energies which apply to the levels involved in the transition marked in Fig. 1. Designating the levels by the numbers shown on the right of Fig. 1, we have

$$\psi(F,m) = \sum_{m_J, m_I} (Fm|m_J m_I)\phi(m_J)\chi(m_I),$$

$$\psi_1 \equiv \psi(\tfrac{3}{2}, \tfrac{3}{2}) = \phi(\tfrac{1}{2})\chi(1),$$

$$\psi_2 \equiv \psi(\tfrac{3}{2}, \tfrac{1}{2}) = a\phi(\tfrac{1}{2})\chi(0) + b\phi(-\tfrac{1}{2})\chi(1),$$

$$\psi_3 \equiv \psi(\tfrac{3}{2}, -\tfrac{1}{2}) = c\phi(\tfrac{1}{2})\chi(-1) + d\phi(-\tfrac{1}{2})\chi(0), \quad (2)$$

$$\psi_4 \equiv \psi(\tfrac{3}{2}, -\tfrac{3}{2}) = \phi(-\tfrac{1}{2})\chi(-1),$$

$$\psi_5 \equiv \psi(\tfrac{1}{2}, -\tfrac{1}{2}) = c\phi(-\tfrac{1}{2})\chi(0) - d\phi(\tfrac{1}{2})\chi(-1),$$

$$\psi_6 \equiv \psi(\tfrac{1}{2}, \tfrac{1}{2}) = a\phi(-\tfrac{1}{2})\chi(1) - b\phi(\tfrac{1}{2})\chi(0).$$

The coefficients, as functions of $x = (g_J - g_I)\mu_0 H_0/h\Delta\nu$, will be expressed in terms of $r = (1 + \frac{4}{3}x + x^2)^{\frac{1}{2}}$ and $\rho = (1 - \frac{2}{3}x + x^2)^{\frac{1}{2}}$:

$$a^2 = \frac{1}{2} + \left(\frac{1}{4} - \frac{2}{9r^2}\right)^{\frac{1}{2}}, \quad c^2 = \frac{1}{2} + \left(\frac{1}{4} - \frac{2}{9\rho^2}\right)^{\frac{1}{2}},$$

$$b^2 = \frac{1}{2} - \left(\frac{1}{4} - \frac{2}{9r^2}\right)^{\frac{1}{2}}, \quad d^2 = \frac{1}{2} - \left(\frac{1}{4} - \frac{2}{9\rho^2}\right)^{\frac{1}{2}}. \quad (3)$$

The energy levels of Fig. 1 are given by

$$W_{F=1,\frac{1}{2}} = -\tfrac{1}{6}h\Delta\nu + g_I\mu_0 H_0 m$$
$$\pm\tfrac{1}{2}h\Delta\nu[1 + (4/3)mx + x^2]^{\frac{1}{2}}. \quad (4)$$

The experiments to be discussed in Sec. 8 involve excitation of transitions between levels 3 and 4 of Fig. 1 at a frequency,

$$\nu_{43} = \Delta\nu\{-\tfrac{1}{2}(1-x) + \tfrac{1}{2}(1 - \tfrac{2}{3}x + x^2)^{\frac{1}{2}}\} + g_I\mu_0 H_0/h, \quad (5)$$

of 60 Mc/sec, which corresponds to an external magnetic field of about 31.4 oersteds. Values of the coefficients of Eqs. (3) for this field are listed below:

$$a^2 = 0.950, \quad b^2 = 0.050, \quad c^2 = 0.903, \quad d^2 = 0.097,$$
$$x = g_J\mu_0 H_0/h\Delta\nu = 1.610.$$

For the $ON(SO_3)_2^{--}$ ion, $g_I/g_J \approx 10^{-4}$ and we shall usually neglect g_I in comparison with g_J.

2. PARAMAGNETIC RELAXATION AND SPIN SATURATION

Paramagnetic relaxation is the process of energy exchange between an assembly of paramagnetic spins and its surroundings which permits the spin-state populations to adjust themselves to the equilibrium distribution corresponding to a given magnetic field and temperature. It is customary to regard the entire paramagnetic sample (solid, liquid, or gas) as a super system composed of two weakly interacting subsystems; the system of interest or spin system, having spin coordinates among its degrees of freedom, and the surroundings or lattice system having only orbital degrees of freedom.

It is the weak interaction, $\mathcal{H}_{sl}$, between spins and the lattice which is the object of relaxation studies. In practical cases, the question is one of trying to discover which of a number of possibly important spin-lattice interactions effects the experimentally observed relaxation. In certain examples relaxation has been studied experimentally through direct observation of the characteristic time required for the establishment of spin equilibrium (the *relaxation time*). In other examples, particularly if the relaxation time is short, one measures essentially the thermal conductivity between the spins and the lattice by observing the rate at which energy, absorbed by the spins from a laboratory source, is passed on to the lattice via the relaxation mechanisms; this is the saturation method.

It is of course quite feasible to cloak such measurements in thermodynamic terms, as was done by Casimir and Du Pré.[6] We shall usually confine our approach to that of quantum statistics and speak in terms of the transition probabilities per unit time induced by $\mathcal{H}_{sl}$. Either a direct relaxation time measurement or a saturation experiment will be treated in terms of the

[6] H. B. G. Casimir and F. K. Du Pré, Physica 5, 507 (1938); H. B. G. Casimir, Physica 6, 159 (1939).

way in which the populations of the various energy states are influenced by these probabilities.

Such an analysis of the relaxation time for an assembly of spin $\frac{1}{2}$ particles is straightforward;[7] a unique relaxation time is easily defined for the establishment of the equilibrium population difference between the two spin states accessible to each particle. However, a more complicated energy level scheme may not permit the association of a single relaxation time with each *pair* of levels between which a population difference will exist at equilibrium. An example is the coupled system consisting of the odd electron and the N^{14} nucleus of the free-radical ion $ON(SO_3)_2^{--}$. Not only are there six unevenly spaced levels, but the selection rules permit magnetic dipole transitions between all but five of the fifteen different pairs of levels. In general, one finds that the approach, from an initially disturbed state to the equilibrium level population, is described by an expression of the form

$$N_k(t) = \sum_l b_{kl} \exp(-\lambda_l t). \quad (6)$$

If, after appreciable lapse of time, several comparable terms in the sum (6) are dominant, it will be impossible to express any population difference involving level k with only one exponential term, and there will be no single relaxation time.

The saturation procedure does not suppose any specific mathematical form for the approach to equilibrium of the population difference between a pair of levels. Transitions are excited between the levels in question by means of a laboratory radiation field. (We presume throughout this discussion the existence of a constant external magnetic field which removes the orientation degeneracy of individual spins.) As we shall later verify (Sec. 4), the transition probabilities induced by the laboratory field are, for practical purposes, microscopically reversible, which means that the net energy absorption—and therefore also the detected rf absorption signal—is proportional to the population difference. In the presence of a given laboratory radiation field, then, a stationary spin population distribution will ultimately obtain in which this rf absorption is just balanced by the energy carried to the lattice through all relaxation processes. (As taken up in Sec. 5, the transition probabilities describing the relaxation processes *cannot* possess microscopic reversibility if there is to be a nonvanishing population differential at equilibrium.) It follows that a study of relative absorption intensity as a function of the rf power level must give direct information about the interaction $\mathcal{3C}_{sl}$ which permits energy exchange between the spins and the lattice.

Explicit emphasis should perhaps be given to the fact that a given level of saturation is characterized by *stationarity* of spin population, but not, of course, by thermal equilibrium. Indeed, the stationarity exists

[7] Bloembergen, Purcell, and Pound, Phys. Rev. 73, 679 (1948), often referred to hereafter as BPP.

only if the thermal capacity of the lattice, which is in turn normally in excellent thermal contact with its laboratory surroundings, is large. Except at very low temperatures, this condition is usually fulfilled. For this reason, although there is a steady flow of energy into the lattice, we shall speak of a lattice temperature, assumed not to change during a given measurement, which is essentially a temperature fixed by the sample's immediate laboratory surroundings.[8]

3. DEFINITION OF THE SATURATION FACTOR AND THE RELAXATION PROBABILITY

The foregoing description of the saturation procedure suggests that a useful quantity in relaxation studies is the ratio,

$$S_{jk}(H_1) = (N_k' - N_j')/(N_k - N_j), \quad (7)$$

which we shall call the saturation factor. Here N_k is the stationary population of spin state k with zero or negligible rf field present (thus the thermal equilibrium value) and N_k' is the stationary population in the presence of an rf field H_1. Evidently $S_{jk}(0) = 1$ and $S_{jk}(\infty) = 0$. For a given input of rf power at spin resonance, one expects S_{jk} to depend upon lattice temperature and the external field in which resonance occurs.

We now wish to obtain a relationship which expresses the saturation factor in terms of the laboratory-induced transition probability per unit time V_{jk}, and the transition probability per unit time U_{jk} which is induced by the spin-lattice interaction $\mathcal{3C}_{sl}$. We shall let $W_{jk} = U_{jk} + V_{jk}$ denote the probability per unit time, due to both relaxation mechanisms and the laboratory apparatus, that a system now in spin state j will be found at a later time in state k. If there are a total number N of spin systems to be distributed over the n states accessible to an individual spin, then the following differential equations describe the shifting of the population fractions, $Q_j = N_j/N$, by expressing essentially the conservation of systems:

$$\frac{dQ_j}{dt} = \sum_{\substack{k=1 \\ k \neq j}}^{n} (Q_k W_{kj} - Q_j W_{jk}) \quad [j = 1, \cdots, n]. \quad (8)$$

Under conditions of population stationarity, Eqs. (8) become n homogeneous linear equations in the Q's which are readily seen to be consistent, since any row of their coefficient determinant is obtainable by adding the other $n-1$ rows. The Q's are of course not all independent, for if $n-1$ of them are known, the nth is determined. Thus the system of equations may be solved by replacing any one of the n homogeneous equations,

$$\sum_{\substack{k=1 \\ k \neq j}}^{n} (Q_k W_{kj} - Q_j W_{jk}) = 0 \quad [j = 1, \cdots n], \quad (9)$$

[8] In the early unsuccessful attempt of Gorter to observe nuclear paramagnetic resonance, the small change of lattice temperature during application of a strong rf field at the Larmor frequency was to be the means of detecting the nuclear spin resonance [C. J. Gorter, Physica 3, 995 (1936)].

by

$$\sum_{k=1}^{n} Q_k = 1. \tag{10}$$

To determine the saturation factor S_{qp}, we require the difference $\Delta_{pq} = Q_p - Q_q$ under the conditions,

$$
\left.
\begin{aligned}
W_{jk} &= U_{jk} \qquad [qp \neq jk \neq pq] \\
W_{pq} &= U_{pq} + V \\
W_{qp} &= U_{qp} + V
\end{aligned}
\right\}, \tag{11}
$$

which express the reversibility of $V_{pq} = V_{qp} = V$ and the fact that the laboratory source induces transitions between states p and q only.

For simplicity, let us arbitrarily number the states p and q, between which the radiation field produces transitions with the probability V, by the numbers 1 and 2. Then, substituting $Q_2 = \Delta_{21} + Q_1$, one obtains the following equations:

$$
\begin{aligned}
&Q_1\left[U_{21} + V - (V + \sum_k U_{1k})\right] + \Delta_{21}(U_{21} + V) \quad + Q_3 U_{31} + \cdots + Q_n U_{n1} = 0, \\[4pt]
&Q_1\left[U_{12} + V - (V + \sum_k U_{2k})\right] - \Delta_{21}(V + \sum_k U_{2k}) + Q_3 U_{32} + \cdots + Q_n U_{n2} = 0, \\[4pt]
&\qquad\qquad \vdots \\
&Q_1(U_{1m} + U_{2n}) \qquad\qquad + \Delta_{21} U_{2m} \qquad\quad + Q_3 U_{3m} + \cdots + Q_n U_{nm} = 0, \\[4pt]
&\qquad\qquad \vdots \\
&Q_1(U_{1n} + U_{2n}) \qquad\qquad + \Delta_{21} U_{2n} \qquad\quad + Q_3 U_{3n} \cdots - Q_n \sum_k U_{nk} = 0.
\end{aligned} \tag{12}
$$

Noting that V, by virtue of its practical microscopic reversibility, appears only in two positions in the second column, one can eliminate one V term by replacing, for example, the second equation by Eq. (10). If one then solves for Δ_{21} by expanding determinants in terms of the cofactors of the second column, he obtains

$$\Delta_{21} = C_{22} / \left(\sum_{k \neq 2} U_{2k} C_{2k} + V \cdot C_{21} + C_{22}\right), \tag{13}$$

where C_{2k} is the cofactor of the second column element in the kth row. For a spin system in thermal equilibrium at room temperature, $\Delta_{21} \sim (E_2 - E_1)/kt = h\nu/kT$. For magnetic dipole transitions which would occur at radio-frequencies between 1 Mc/sec and 30 000 Mc/sec, Δ_{21} ranges between 10^{-7} and 5×10^{-3}. Then Eq. (13) indicates that $\sum_{k \neq 2} U_{2k} C_{2k}$ must exceed C_{22} by a factor at least 200 (and, for the experiments of Sec. 7, by 10^5). Hence C_{22} can be dropped from the denominator of Eq. (13), and one finds $S_{12} = \Delta_{21}(V)/\Delta_{21}(0)$ to be

$$S_{12} = \left[1 + \cfrac{V}{U_{21} + C_{21}^{-1} \sum_{k=3}^{n} U_{2k} C_{2k}}\right]^{-1}. \tag{14}$$

This may be compared with BPP's Eqs. (13), (4), and (33) to show that our result reduces to theirs when there are just two levels. Although a system of many levels without special selection rules does not generally admit to definition of a single relaxation time for a pair of levels, the coefficient of V in Eq. (14), which for a two level system is twice the relaxation time T_1, is nevertheless the significant quantity indicating the potency of relaxation mechanisms which give rise to the U_{jk} transition probabilities. We shall define the reciprocal of the coefficient of V to be the *relaxation probability*, W_R:

$$W_R = U_{21} + \frac{1}{C_{21}} \sum_{k=3}^{n} U_{2k} C_{2k}. \tag{15}$$

We can thus speak of measuring relaxation probabilities in situations where there is no single uniquely defined relaxation time.[9]

4. THE LABORATORY-INDUCED TRANSITION PROBABILITY

Experimental measurement of W_R can be made by measuring S for a known rf field and using the result of Eqs. (14) and (15),

$$S = [1 + V/W_R]^{-1}, \tag{16}$$

once we know how V depends upon the rf field.

The probability V_{jk} is often calculated from the semiclassical perturbation treatment of radiation,[10] in which event one assumes the existence of zero-order spin functions u_n, which satisfy the eigenvalue equation

$$\mathcal{H}_s u_n = E_n u_n, \tag{17}$$

and a perturbing interaction,

$$\mathcal{H}' = A[e^{i\omega t} + e^{-i\omega t}] = 2A \cos\omega t. \tag{18}$$

In our case of particular interest in magnetic dipole

[9] To the extent that Bloch's phenomenological equations [Phys. Rev. 70, 460 (1946)] adequately represent the motion of the magnetization vector associated with a particular spin system, the time T_1 describing the exponential decay of that magnetization will, of course, be a perfectly useful parameter. However, one cannot assert generally that the Bloch T_1 bears any simple relationship to the λ's of Eq. (6). Special cases in which the Bloch parameters are rigorously related to microscopic quantities are discussed by R. K. Wangsness and F. Bloch [Phys. Rev. 89, 728 (1953)].

[10] See, for example, L. I. Schiff, *Quantum Mechanics* (McGraw-Hill Book Company, Inc., New York, 1949), Secs. 29 and 35.

transitions, A may arise from an interaction $-\boldsymbol{\mu}\cdot\mathbf{H}$ where $\mathbf{H}$ is the field of the oscillator used in the laboratory to cause spin resonance. Then the usual time-dependent perturbation calculation yields the following first-order expression for the probability that the system, initially in a state j, will be found in state k:

$$|a_k(t)|^2 = h^{-2}|\langle k|A|j\rangle|^2 \frac{4\sin^2[\frac{1}{2}(\omega_{kj}-\omega)]}{(\omega_{km}-\omega)^2}. \quad (19)$$

For times not too short,

$$\frac{4\sin^2[\frac{1}{2}(\omega_{kj}-\omega)t]}{(\omega_{kj}-\omega)^2} = t\cdot\delta(\nu_{kj}-\nu), \quad (20)$$

and the probability per unit time is

$$V_{j\to k} = h^{-2}|(k|A|j)|^2\delta(\nu_{kj}-\nu). \quad (21)$$

If we take $\mathcal{H}' = -\mu_x(2H_1)\cos(\omega t)$ and suppose that the spin resonance frequencies of the individual spins of the sample are distributed over a finite frequency range according to a normalized line shape function $g(\nu)$, then

$$V_{jk} = h^{-2}H_1{}^2|(k|\mu_x|j)|^2 g(\nu). \quad (22)$$

The V_{jk} so obtained is of necessity microscopically reversible, because μ_x is Hermitian.

If, however, the quantum nature of the radiation field is taken into account, the probability of absorptive transition is proportional to the mean number of photons $n(\nu)$ per degree of freedom of the field coordinates belonging to waves of frequency ν. If $\rho(\nu)d\nu$ is the energy density of the field per unit volume in the frequency range $d\nu$, then[11]

$$n(\nu) = \frac{c^3}{8\pi h\nu^3}\rho(\nu). \quad (23)$$

The quantum treatment of emission shows it to be proportional to $n(\nu)+1$, thus including in the theory the spontaneous emission probability (when $n(\nu)=0$) arrived at by Einstein from statistical considerations of thermal equilibrium. To test the effective reversibility of emission and absorption probabilities, we evaluate $[n(\nu)+1]/n(\nu)$ for the signal generator, assuming it to produce an rf field of about 0.1 gauss in a frequency interval of at most 100 cycles/sec at 6×10^7 cycles/sec. One finds from Eq. (23) that $n(\nu)$ is at least 10^{25}. Then clearly, to the extent that $n(\nu)+1\cong n(\nu)$, we may consider that $V_{jk}=V_{kj}$ even when the quantum nature of our laboratory radiation field is taken into account. We shall use for either V_{jk} or V_{kj} the semiclassical result (22) which, since it is proportional to $H_1{}^2$ and includes no possibility of spontaneous emission, must correspond to the actual *absorption* probability.

[11] E. U. Condon and G. Shortley, *Theory of Atomic Spectra* (Cambridge University Press, Cambridge, 1935), p. 80.

5. THE TRANSITION PROBABILITIES EFFECTING RELAXATION

The application of perturbation theory to the calculation of transitions induced by $\mathcal{H}_{sl}$ is, in principle, straightforward. One treats $\mathcal{H}_{sl}$ as a perturbing interaction for the zero-order Hamiltonian,

$$\mathcal{H}_0 = \mathcal{H}_s + \mathcal{H}_l, \quad (24)$$

where $\mathcal{H}_s$ and $\mathcal{H}_l$ are, respectively, the spin and lattice Hamiltonians. In practice, however, even the assembly of spins, which may often be considered as noninteracting among themselves, offers a highly degenerate system for which the orthonormal zero-order linear combinations are not known, nor are the normal modes for the lattice. The classic example of a serious effort to take into account the normal modes for a particular lattice is Van Vleck's calculation of the relaxation times for titanium and chrome alums.[12]

Our experiments deal with liquids, for which there is available almost no information on "lattice" eigenstates. Bloembergen, Purcell, and Pound[7] have, however, obtained excellent results for nuclear paramagnetic relaxation in liquids by approaching the problem from the point of view of the correlation spectrum. The procedure is effectively one of using the semiclassical perturbation treatment for the effect of an oscillatory magnetic field component which might arise through translational or rotational motions of the charges associated with molecules of the liquid; these frequency components are then taken to be distributed according to the correlation spectrum. We can illustrate this procedure by taking A of our Eq. (18) as a product (or as a sum of products), one factor containing (lattice) space coordinates and the other dependent upon particle angular momentum operators,

$$A = f(\mathbf{r})F_{op}(\mathbf{I},\mathbf{J}). \quad (25)$$

Then Eq. (19) becomes

$$U_{j\to k} = h^{-2}|f(\mathbf{r})|^2|(k|F_{op}|j)|^2\delta(\nu_{kj}-\nu). \quad (26)$$

The correlation theory for liquids leads to the conclusion that $|f(\mathbf{r})|^2$ is distributed spectrally according to the intensity,[7]

$$J(\nu) = \langle|f(\mathbf{r})|^2\rangle_{Av}\frac{2\tau_c}{1+4\pi^2\nu^2\tau_c{}^2}, \quad (27)$$

where τ_c is the correlation time and the average is over all time or, equivalently, over all space if $f(\mathbf{r})$ is a function of coordinates which vary randomly with time. Combining Eqs. (26) and (27), one obtains

$$U_{jk} = h^{-2}\langle|(k|f(\mathbf{r})F_{op}(\mathbf{I},\mathbf{J})|j)|^2\rangle_{Av}j(\nu_{kj}), \quad (28)$$

where $j(\nu)$ is the normalized spectrum

$$j(\nu) = \frac{2\tau_c}{1+4\pi^2\nu^2\tau_c{}^2}. \quad (29)$$

[12] J. H. Van Vleck, Phys. Rev. 57, 426 (1940).

We now ask to what extent a proper quantum approach, analogous to Van Vleck's for the alums, would yield significant features not present in this semiclassical result.

Following the procedure of Sommerfeld and Bethe,[13] for example, we would prefer to have quantized the normal modes of the lattice. The lattice states would then be described by a set of quantum numbers n_i for the ith mode of elastic waves. The energy of the quantized mode is given by $(n_i+\frac{1}{2})\hbar\omega_i$, and energy exchange between such modes and the spins may be described as either emission or absorption of a "phonon" of energy $\hbar\omega_i$ by the spin system. The formalism is quite parallel to that for the radiation field, including the fundamental asymmetry between emission and absorption. The probability of emission (creation) of a phonon of frequency ω_i by the spin system is proportional to n_i+1, whereas that of absorption (annihilation) is simply proportional to n_i.

If the lattice temperature is T, the mean value of n_i is

$$\bar{n}_i = \frac{1}{\exp(\hbar\omega_i/kT)-1}, \qquad (30)$$

so that emission and absorption probabilities are in the ratio

$$\frac{U_{\text{emission}}}{U_{\text{absorption}}} = \frac{\bar{n}_i+1}{\bar{n}_i} = \exp(\hbar\omega_i/kT). \qquad (31)$$

As with the semiclassical treatment of the radiation field, Sec. 4, the semiclassical result (28) is microscopically reversible and is proportional to the intensity of the effective phonon field. We again identify the semiclassical result with the absorption probability of a full quantum treatment, and the emission probability is to be calculated from Eq. (31). Thus, if spin state k has greater energy than state j,

$$U_{j\to k} = \hbar^{-2}\langle|(k|f(\mathbf{r})F_{op}(\mathbf{I,J})|j)|^2\rangle_{Av}j(\nu_{kj})$$
$$U_{k\to j} = U_{j\to k}e^{\hbar\nu_{kj}/kT}. \qquad (32)$$

Note that Eq. (32) disagrees with BPP's Eq. (30) (which is for the special case of spin $\frac{1}{2}$). Although the BPP equation gives the proper ratio of emission and absorption probabilities, each depends upon the zero of the energy scale used in measuring E_p and E_q of BPP Eq. (29).

The distinction between solids and liquids, so far as application of Eq. (32) is concerned, lies in the selection of $j(\nu)$. It may be, for a solid, the normalized Debye spectrum of the familiar classical theory of the specific heat, or, for a liquid, it may be the correlation spectrum (29). The essential parameter in the first case is the Debye temperature, whereas in the second it is the correlation time.

---

[13] A. Sommerfeld and H. Bethe, *Handbuch der Physik* (Springer, Berlin, 1933), second edition, Vol. 24/2, p. 500 ff.

5. DETAILED BALANCE AND SPIN SATURATION

If spin state k has higher energy than state j, then at thermal equilibrium the principle of detailed balance,

$$N_k U_{kj} = N_j U_{jk}, \qquad (33)$$

combines with Eq. (31) to assure a Boltzmann distribution among the spin states.

It is interesting to raise the question whether the principle of detailed balance applies to the spin system in a partially saturated state. Treatises on statistical mechanics often arrive at detailed balance by a classical argument, and none which has come to the authors' attention is clear in a quantum statistical way on whether detailed balance is applicable outside of thermal equilibrium. For our particular problem, the assumption of detailed balance outside thermal equilibrium appears to lead to a contradiction, as is perhaps most easily illustrated for three levels between any pair of which the selection rules for the interaction effecting relaxation permit transitions.

If N_1, N_2, and N_3 are the level populations, then the steady state solution of Eqs. (9) and (10) under conditions of detailed balance leads to an expression for N_1-N_2 which can be cast into the form

$$N_1 - N_2 = N\frac{W_{23}W_{31}-W_{13}W_{32}}{W_{13}W_{32}+W_{13}W_{23}+W_{31}W_{23}}. \qquad (34)$$

Now suppose a monochromatic radiation field inducing transitions between 1 and 2 is introduced. Then $W_{12}=U_{12}+V$ and $W_{21}=U_{21}+V$ will be altered, and the other W's remain simply the corresponding U's. We know experimentally that increasing $V_{12}=V_{21}=V$ enables us to diminish N_1-N_2 as much as we please. Yet, by assuming detailed balance, we expressed N_1-N_2 independently of W_{12} and therefore of V.

Another way of making this point is to observe that detailed balance requires the condition

$$W_{12}W_{23}W_{31} = W_{21}W_{32}W_{13}, \qquad (35)$$

which becomes, for no rf field,

$$U_{12}U_{23}U_{31} = U_{21}U_{32}U_{13}. \qquad (36)$$

If $V_{12}=V_{21}=V$ is impressed with an external radiation field, then (35) becomes

$$(U_{12}+V)U_{23}U_{31} = (U_{21}+V)U_{32}U_{13}, \qquad (37)$$

which cannot hold for all V if $U_{21}\neq U_{12}$.

Of course, the arguments of this section do not include explicit account of direct interaction between the rf field and the lattice. Although this is usually extremely weak, and is considered not to affect the lattice energy states nor their populations, the U's are in principle altered by this perturbation and a convincing demonstration would have to verify that the U's are not so altered as to keep Eq. (37) always valid. Our argument is essentially that V can be and is made

comparable to or greater than U_{12}, whereas the radiation field-lattice interaction should affect the U's only by a very small (negligible, we think) fraction.

In the analysis of Sec. 3, therefore, the simple conservation of systems, as described by Eqs. (9) and (10), and the assumption that the presence of V does not alter the U's are used to obtain the saturation factor. There is no question of applying detailed balance, since it is violated by these assumptions.

7. APPARATUS AND EXPERIMENTAL PROCEDURE

Figure 2 is a block diagram of the apparatus used to produce the transitions, detect the resonance, and measure the saturation factor S. The 60-Mc/sec rf field is produced in the tank coil of a Colpitts-type oscillator which forms part of a magnetic resonance spectrometer similar in design to that of Schuster.[14] Audio amplifiers with a total gain of about a million followed the resonance detector and fed a phase-sensitive detector.[15]

A 30-cycle signal generator produced a square wave reference signal for the phase-sensitive detector and a synchronized sinusoid which, after power amplification, modulated the Helmholtz coil field of about 30 oersteds. This generator also supplied the 30-cycle signal to the grid of the calibrator,[16] a device which essentially places the plate resistance of a triode, type 955 in this case, across the oscillator tank coil to provide dissipation which simulates a nonsaturable signal serving as a comparison standard for the paramagnetic sample.

In order to know the transition probability (22) produced by the oscillator for a given sample, one requires the half-amplitude H_1 of the rf field at the sample. For this purpose a vacuum tube voltmeter was built into the apparatus to measure the rms voltage v across the sample coil. The inductance of the coil, which was wound of small flat copper strap to minimize

FIG. 2. Block diagram of the experimental arrangement.

[14] N. A. Schuster, thesis, Washington University, 1951 (unpublished).
[15] N. A. Schuster, Rev. Sci. Instr. 22, 254 (1951).
[16] G. D. Watkins and R. V. Pound, Phys. Rev. 82, 343 (1951). The authors are indebted to Dr. Watkins for communicating to them further information on his work.

the capacitance between turns, was determined, and the ratio of magnetic field to current in the coil was obtained by performing an auxiliary resonance experiment for which a direct current through the coil produced the external magnetic field for a still smaller coil containing a free radical. The result so obtained is that

$$H_1 = 0.022v. \qquad (38)$$

A typical measurement of the saturation factor might proceed as follows. The plate voltage of the oscillator is adjusted to provide a low level of oscillation, and the calibrator is set to give a signal equal to that obtained from the paramagnetic sample. The level of oscillation is then increased and a new comparison of calibrator and sample signals is made. In general, the power level and changes in the properties of the oscillator circuit at the new oscillation level will alter the absolute signal intensity, but these changes will affect equally the signal from a given dissipative load across the coil, whether of paramagnetic or calibrator origin, and the relative intensity is meaningful. If the calibrator and the sample still produce the same relative signal, then S is still unity and saturation has not set in. The oscillation level is then further increased until a curve
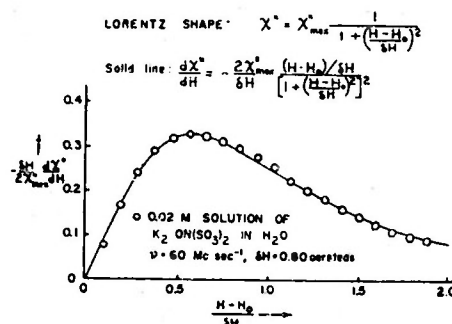

FIG. 3. Comparison of experimental absorption derivative points with the first derivative of a Lorentz shape function. To obtain the entire absorption derivative, the curve shown should be reflected in the origin.
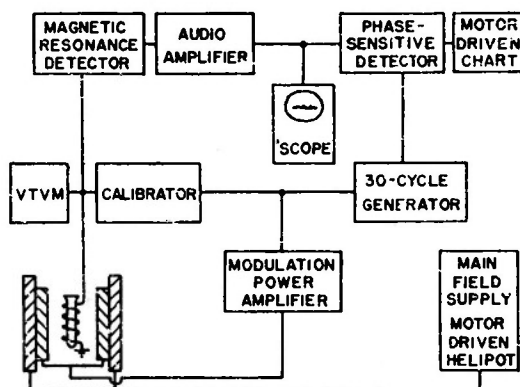
of S versus v, the rms coil voltage, is plotted; by means of Eq. (38) such a curve can be converted to S versus H_1.

The shape function $g(\nu)$ required to calculate V_{jk} from (22) is determined from the measured resonance curves at low power (where $S = 1$). Since the modulation technique is used, the line profile actually measured is proportional to the derivative $dg/d\nu$. Of course, the calibrator triode is supplied with a 30-cycle grid signal to provide a standard signal coherent with the phase-sensitive detector reference voltage.

8. EXPERIMENTAL RESULTS

Aqueous solutions of $K_2ON(SO_3)_2$ are unstable and often become diamagnetic in a matter of several minutes, the decay products catalyzing the spin-pairing reaction. It was found that making the solution about
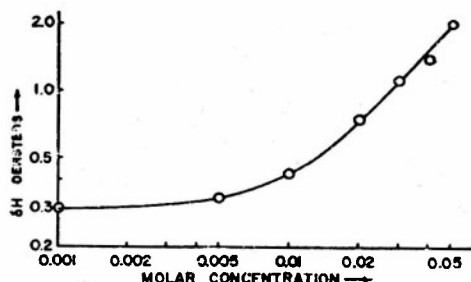
FIG. 4. Experimental line width *versus* concentration of $ON(SO_3)_2^{--}$ ion in aqueous solution. The quantity δH is defined in Fig. 3.

0.1 normal in Na_2CO_3 stabilizes the free radical solution in a pH range proper to prevent appreciable deterioration for several days.[17] In this way, measurements were easily made on samples containing various concentrations of $ON(SO_3)_2^{--}$ ion.

All measurements reported here were made at 60 Mc/sec for the transition $(F=\frac{3}{2}, m_F=-\frac{3}{2})\leftrightarrow(F=\frac{3}{2}, m_F=-\frac{1}{2})$, which is transition $4\leftrightarrow3$ on Fig. 1. This transition was selected because its frequency *versus* field characteristic does not depart sufficiently from linearity to complicate width measurements, as may happen for those transitions having small $d\nu/dH$, and because it is reasonably intense. This transition gives, at a fixed microwave frequency, the hyperfine triplet which occurs in the highest external field.

Figure 3 graphs experimental points for half of the derivative curve of the resonance absorption of a $0.02M$ aqueous solution of $ON(SO_3)_2^{--}$ at 60 Mc/sec. Also placed on the graph field is a curve corresponding to the derivative of a so-called Lorentz[18] or damped-oscillator line shape function. It is seen that the Lorentz curve approximates very well to the experimental points.

In our analysis of the experimental saturation data, we follow BPP, whose equations[19] can be adapted to show that for our situation (BPP case I: the modulation frequency is much less than W_R) the decline in the derivative extremum under saturation is given by a saturation factor,

$$S' = \frac{d\chi''(H_1)}{d\nu}\bigg/\frac{d\chi''(H_1\to0)}{d\nu} = [1+V/W_R]^{-\frac{3}{2}} = S^{\frac{3}{2}}. \quad (39)$$

Note that S' is not a derivative of S. The value of V to be used in this expression is its maximum at the resonance center, thus corresponding to the maximum value of $g(\nu)$. For a Lorentz line, $g(\nu)_{max}$ is $1/\pi$ times the reciprocal of the half-width $\delta\nu$ at half-maximum intensity on the unsaturated $g(\nu)$ curve. If one measures experimentally the width, in magnetic field units,

[17] We are indebted to Professor Weissman of the Washington University department of chemistry for this discovery.
[18] G. E. Pake and E. M. Purcell, Phys. Rev. 74, 1184 (1948).
[19] Reference 7, Sec. IV, Eq. (17). The BPP saturation parameter s is our V/W_R.

between points of extreme slope, the conversion between the measured quantity ΔH and $g(\nu)_{max}$ is, for the Lorentz shape function shown on Fig. 3,

$$g(\nu)_{max} = (4/\sqrt{3})(\gamma\Delta H)^{-1}, \quad (40)$$

where $\gamma=d\omega/dH$ is obtained from the (angular) frequency *versus* field characteristic for the transition in question. The parameter δH of Fig. 3 is, in terms of the width between inflection points, $(\sqrt{3}/2)\Delta H$.

Figures 4 and 5 plot, respectively, the experimental values of δH and of the relaxation probability W_R *versus* the molar concentration of $ON(SO_3)_2^{--}$ ion. At concentrations above $0.05M$, the hyperfine structure begins to give way to a single broad line. The lower limit of the concentration range is determined by the decline in signal sensitivity as fewer and fewer free radicals are present in the sample.

A striking feature of Figs. 4 and 5 is that both the line width and relaxation probability appear to approach
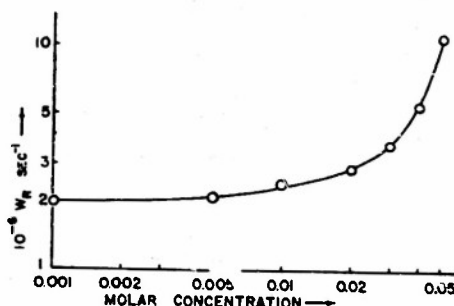

FIG. 5. Experimental relaxation probability W_R *versus* concentration of $ON(SO_3)_2^{--}$ ion in aqueous solution.

asymptotically a concentration independent value. The relaxation probability, through its limitation of the lifetime of a spin state, should contribute an amount the order of W_R/γ to the total line width. The low-concentration value of W_R/γ gives about 0.7 oersted. This is quite comparable to the asymptotic low-concentration line width of 0.3 oersted, and it indicates that the relaxation processes may well determine the entire line width. If such is the case, we will understand the low-concentration portion of both Figs. 4 and 5 if we can explain the concentration independent relaxation probability.[20]

In order to test the possibility that the nuclear moments of the water solvent might provide the interaction which relaxes the free radical spins, the low-

[20] Depending upon the relationship which one assumes should exist between W_R and its contribution to δH, the fact that W_R/γ *exceeds* δH may cause some concern for the internal consistency of our measurements; the line cannot be sharper than the uncertainty principle would allow. However our procedure of calibrating the rf coil (Sec. 7) when it carries direct current is not beyond reproach, inasmuch as the current distribution throughout the cross section of the copper strap at 60 Mc/sec is certainly somewhat different from the dc distribution. Therefore a factor of perhaps 2 must be allowed in our absolute values of W_R; relative values should be good within 10 percent or better.

concentration measurements of Figs. 4 and 5 were made for solutions of $ON(SO_3)_2^{--}$ in D_2O. Although the deuteron magnetic moment is about 0.3 that of the proton, the curves for the D_2O solution were indistinguishable from those of Figs. 4 and 5. We thus have experimental indication that the nuclear moments of the solvent do *not* provide the relaxation mechanism.

9. THE SATURATION FACTOR FOR THE TRANSITION STUDIED

In order to compare postulated relaxation mechanisms with the measured value of W_R, we require the expression for W_R in terms of the U's for $ON(SO_3)_2^{--}$. There are six homogeneous equations of the form (9) for a system with the energy levels of Fig. 1. For magnetic dipole transitions in the radio-frequency range, the Boltzmann factors associated with emission [Eq. (31)] usually depart from unity by less than 10^{-4}. Furthermore, BPP finds for water at room temperature that $\tau_c = 4 \times 10^{-2}$ sec. In 31.4 oersteds, all transitions permitted between the levels of Fig. 1 occur at frequencies of 10^7 or 10^8 sec^{-1}. By Eq. (29), the resulting correlation spectrum $j(\nu)$ is essentially "white" with intensity $2\tau_c$ per unit frequency range.

Comparison of relative values of the coefficients in the six homogeneous equations may therefore be made from

$$U_{jk} = \hbar^{-2} \langle f(\mathbf{r})^2 \rangle_{Av} |(k|\mathbf{\mu}|j)|^2 2\tau_c, \tag{41}$$

in which the operator function F_{op} of Eq. (28) is

$$\mathbf{\mu} = -g_J \mu_0 \mathbf{J} + g_I \mu_0 \mathbf{I} \cong -g_J \mu_0 \mathbf{J}, \tag{42}$$

and its matrix elements are to be calculated using the spin functions (2) which apply for 31.4 oersteds. Such nonvanishing values of $|(k|J_z|j)|^2$ for the π transitions and $|(k|J_x|j)|^2$ for σ transitions are tabulated in decreasing order in Table I.

Magnetic dipole transitions between level pairs 1 and 3, 1 and 4, 1 and 5, 2 and 4, and 4 and 6 are forbidden. In addition we shall neglect the three weakest permitted transitions (3 to 6, 5 to 6, and 1 to 2) in solving for S_{43}. After so doing, one finds for S_{43} an equation of the type of Eq. (15) with W_R (43) given by

$$W_R(43) = U_{43} + U_{45}$$

$$\times \frac{U_{25}U_{36} + U_{23}U_{26} + U_{26}U_{35}}{U_{23}U_{36} + U_{23}U_{46} + U_{23}U_{26} + U_{26}U_{46} + U_{26}U_{35}}. \tag{43}$$

Here we have dropped "thermal differences," i.e., $U_{jk} - U_{kj}$, in comparison with U_{il}; this may be done as soon as the equations are placed in a form corresponding to Eq. (12) and it greatly simplifies solution.[21]

---

[21] It is useful to note that the form of the equations and the fact that W_R must depend upon quantities of zero order in "thermal differences" allows one to set up an analogy with a passive network of conductances. Branch points in the analog network correspond to the energy states of the system, and the conductance between j and k corresponds to U_{jk}. This is perhaps the simplest method for calculating W_R in a particular case.

TABLE I. Nonvanishing matrix elements of J_x and J_z connecting the energy states of Fig. 1 are tabulated for a value of x corresponding to 31.4 oersteds. For a "white" correlation spectrum, the respective transition probabilities (41) are proportional to the tabulated numbers.

j	k	$|(k|J_x|j)|^2$	$(k|J_z|j)^2$
3	5		0.350
1	6	0.227	
3	4	0.226	
2	5	0.224	
2	6		0.190
4	5	0.024	
2	3	0.023	
1	2	0.012	
5	6	0.011	
3	6	0.001	

The error in dropping the three weak transitions is evidently not serious, since the correction to U_{43} in Eq. (43) is, for an isotropic white radiation bath, easily shown from the table to be about 10 percent of U_{43}. Errors of 10 percent or so can easily creep into saturation measurements of W_R.

10. THE RELAXATION MECHANISM AT THE HIGHER CONCENTRATIONS

At the high-concentration end of the curves of Figs. 4 and 5, one expects ion-ion collisions to effect relaxation and W_R should be proportional to concentration. Experimentally the log-log plot of Fig. 4 approaches a slope measurably greater than unity, which effect, if real, is unexplained. Measurements are in general difficult to make in this region of concentration, since the hyperfine splitting is about to blur into a single broad line, and the tails of the three high-frequency transitions overlap appreciably. The true width of an individual component line is not easily arrived at under such circumstances.

However, as a check on the mechanism, one should obtain an approximately correct order of magnitude for W_R from the BPP Eq. (50), intended to be used to calculate the contribution to W_R for hydrogen nuclei through their interaction with neighboring water molecules:

$$W_R \cong (9/2)\pi^2 g^4 \mu_0^4 \hbar^{-2} \eta N_0 / 5kT. \tag{44}$$

Here η is the viscosity, which we take for our solution to be that of water at room temperature, about 10^{-2} cgs units. For 0.05 molar, N is 3×10^{19} cm^{-1} and Eq. (44) gives $W_R = 1.5 \times 10^7$ sec^{-1}.

The measured value is $W_R = 1.3 \times 10^7$ sec^{-1}. This is probably adequate agreement considering that we have made the approximation of free electrons by neglecting the nuclear moment coupling and that we have approximated the viscosity of the $ON(SO_3)_2^{--}$ ion.

11. INTERACTION WITH THE NUCLEAR MOMENTS OF THE SOLVENT

Although both D_2O and H_2O had the same effect as solvents, we shall estimate the contribution to W_R to

be expected for this mechanism and check the theory by noting whether the result is negligible in comparison with our measured W_R.

The dipole interaction between the ith hydrogen nucleus of the solvent and the jth ionic spin is

$$\mathcal{K}_{ij} = \mathbf{\mu}_i \cdot \mathbf{\mu}_j r_{ij}^{-3} - 3(\mathbf{\mu}_i \cdot \mathbf{r}_{ij})(\mathbf{\mu}_j \cdot \mathbf{r}_{ij})r_{ij}^{-5}, \quad (45)$$

where

$$\mathbf{\mu}_i = g_I \mu_0 \mathbf{I}_i, \quad \mathbf{\mu}_j = -g_J \mu_0 \mathbf{J}_j. \quad (46)$$

Following BPP, we may write

$$\mathcal{K}_{ij} = -g_I g_J \mu_0^2 [A + B + C + D + E + F], \quad (47)$$

where

$$\begin{aligned}
A &= J_{zj} I_{zi}(1 - 3\cos^2\theta_{ij})r_{ij}^{-3}, \\
B &= -\tfrac{1}{2}[J_{+j}I_{-i} + J_{-j}I_{+i}](1 - 3\cos^2\theta_{ij})r_{ij}^{-3}, \\
C &= -\tfrac{3}{2}[J_{zj}I_{+i} + J_{+j}I_{zi}]\sin\theta_{ij}\cos\theta_{ij}e^{-i\phi_{ij}}r_{ij}^{-3}, \\
D &= -\tfrac{3}{2}[J_{zj}I_{-i} + J_{-j}I_{zi}]\sin\theta_{ij}\cos\theta_{ij}e^{+i\phi_{ij}}r_{ij}^{-3}, \\
E &= -\tfrac{3}{4}J_{+j}I_{+i}\sin^2\theta_{ij}e^{-2i\phi_{ij}}r_{ij}^{-3}, \\
F &= -\tfrac{3}{4}J_{-j}I_{-i}\sin^2\theta_{ij}e^{+2i\phi_{ij}}r_{ij}^{-3}.
\end{aligned} \quad (48)$$

Symbols I_{+i} and J_{-j} denote the respective raising and lowering operators: $I_{+i} = I_{zi} + iI_{yi}$ and $J_{-j} = J_{zj} - iJ_{yj}$.

As an example, consider the contribution of term E from a proton at distance r:

$$U_{43}^{(E)}(r) = g_I^2 g_J^2 \mu_0^4 \hbar^{-2} \sum_{m_i, m_i'} G_{m_i}$$

$$\times \langle |(3; m_i'|E|4; m_i)|^2 \rangle_{Av} j\left(\frac{W' - W}{h}\right), \quad (49)$$

where

$$W' = W_3 - g_I \mu_0 H m_i' \quad \text{and} \quad W = W_4 - g_I \mu_0 H m_i$$

We denote by G_{m_i} the fraction of protons in state m_i, and by W_3 and W_4 the energies corresponding to the levels so numbered in Fig. 1. The nuclear contributions to W' and W are necessary to conserve energy for the transitions, but may be neglected in practice. Therefore

$$j[(W' - W)/h] = 2\tau_c,$$

as indicated in Sec. 9.

Apart from terms of order $g_I \mu_0 H / kT$ (about 10^{-9} in 30 oersteds), $G_{m_i} = \tfrac{1}{2}$ for both spin states of the protons within a thin shell at distance r. In order to consider all protons of the solvent, whatever the value of r, we follow BPP by assuming that $\tau_c = r^2/12D$, D being the diffusion constant, and integrating from the distance of closest approach, r_0, throughout the solvent. If there are N_0 solvent protons per unit volume, the contribution of E is

$$U_{43}^{(E)} = g_I^2 g_J^2 \mu_0^4 \hbar^{-2} \tfrac{1}{2} \sum_{m_i, m_i'} |(3; m_i'| -\tfrac{3}{4}J_{+j}I_{+i}|4; m_i)|^2$$

$$\times \langle |\sin^2\theta_{ij}e^{-2i\phi_{ij}}|^2 \rangle_{Av} N_0 \int_{r_0}^{\infty} r^{-6}(2r^2/12D)4\pi r^2 dr. \quad (50)$$

Performing the indicated sums and integrations and taking the averages of the angle functions, one obtains

$$U_{43}^{(E)} = \tfrac{1}{6}\pi g_I^2 g_J^2 \mu_0^4 \hbar^{-2} c^2 N_0 / D r_0. \quad (51)$$

The diffusion constant is presumably not quite the same as for self-diffusion of pure water. However, we postulate a kind of equivalent viscosity, η, related to $r_0 D$ through Stokes law:

$$1/Dr_0 = 6\hbar\eta/kT. \quad (52)$$

Then

$$U_{43}^{(E)} = \pi^2 g_I^2 g_J^2 \mu_0^4 \hbar^{-2} N_0 \eta c^2 / kT. \quad (53)$$

For pure water, $\eta = 10^{-2}$ cgs units near room temperature; lacking any other value, we use this for our solution. From Sec. 1, we find $c^2 = 0.903$. Finally the relaxation probability obtained from Eq. (53) is

$$W_R^{(E)} \cong 3 \times 10^4 \text{ sec}^{-1} \quad (54)$$

for a dilute aqueous solution of $ON(SO_3)_2^{--}$ ion. This result is indeed consistent with the conclusion from comparison of H_2O and D_2O as solvents: the interaction with solvent nuclear dipole moments is negligible in relation to the measured W_R of 2×10^6 sec^{-1}.

12. RELAXATION THROUGH THE N^{14} QUADRUPOLE MOMENT

The odd electron cannot, since it has spin $\tfrac{1}{2}$, possess a quadrupole moment. However, the electron is magnetically coupled to the N^{14} nucleus, and quadrupolar interactions between the N^{14} nucleus and fluctuating electric field gradients within the liquid can in principle relax the electron spins via the magnetic electron-nuclear coupling.

We deliberately overestimate this contribution to W_R by supposing for argument's sake that the entire electric quadrupole interaction of the N^{14} nucleus with fluctuating electric field gradients is effective in relaxing the electron spin. Actually such relaxation can occur only in low magnetic fields where the coefficients b and d entering into the linear combinations (2) of spin functions are appreciable. An order of magnitude upper limit to W_R from this interaction is therefore, following Eqs. (28) and (29),

$$W_R \sim \hbar^{-2}(eQ)^2 \left\langle \left(\frac{\partial^2 \phi}{\partial z^2}\right)^2 \right\rangle_{Av} 2\tau_c, \quad (55)$$

in which Q is the N^{14} quadrupole moment and ϕ is the electric scalar potential at the nucleus.

Accurate theoretical evaluations of a representative component of the electric field gradient have not been made, even for a rigid lattice, and equally little is known about the average square of such a component for a liquid. However, Bloembergen[22] found that the deuteron effected nuclear relaxation in liquid D_2O, and that the electric field gradient has a magnitude essentially that

[22] N. Bloembergen, Thesis, University of Lieden (Martinus Nijhoff, The Hague, 1948).

at 1A or 2A from an electronic charge. For an estimate, we take er^{-3}, with $r = 1A$, as the magnitude of $\partial^2\phi/\partial z^2$. The value of Q for N^{14} is about 10^{-26} cm². Taking $\tau_c \cong 10^{-11}$ sec, one finds that $W_R \sim 10^{+3}$ sec⁻¹, which is again much smaller than the observed value, 2×10^6 sec⁻¹.

13. THE ROLE OF SPIN-ORBIT COUPLING

In 1936, Kronig[23] proposed that unaccountably short relaxation times in certain alums could be explained by considering the important role played by spin-orbit coupling. The modulation of the spin-spin interaction by the lattice vibrations, considered in Waller's pioneering theory[24] of spin-lattice relaxation, proved entirely inadequate to explain observed relaxation times. Another possibility, the modulation of the crystalline Stark splitting by the lattice vibrations, appears at first sight to hold no promise for relaxation in those substances which possess only Kramers degeneracy in the ground state. However, through the spin-orbit coupling, the modulation of the Stark splitting is felt by the spins.

Van Vleck[12] extended and refined Kronig's ideas in his calculation of relaxation times for titanium and chrome alums. Two processes are distinguished. One, the so-called direct process, gives a highly field-dependent relaxation time which ought to apply at a few degrees Kelvin, but was found to be still too large. The second, or Raman, process is effective in zero as well as in nonvanishing external magnetic fields. It depends upon the inelastic scattering of high-energy vibrational quanta by the spin systems, with the spin system absorbing or emitting a vibrational quantum of very low energy relative to the original vibration quantum. Although this is a second-order process compared to the direct process, it is important because the entire elastic spectrum, rather than a narrow portion at its weak end, is called into play. In fact, the Raman process probably dominates at all but the lowest temperatures.

It is a simple matter[23] to illustrate the influence of a spin-orbit term $\lambda L \cdot S$ on Stark orbitals which possess only spin degeneracy. The spin-orbit interaction renders incomplete the quenching of orbital angular momentum by the crystalline electric field, and, as a result, the spectroscopic splitting factor[25] departs from the free electron value, $g_e = 2.0023$, by an amount the order of λ/Δ, where Δ is the Stark interaction.

It is less simple to demonstrate the existence, via the Raman process, of relaxation caused by modulation of the Stark splitting in the presence of the spin-orbit term $\lambda L \cdot S$. In fact, Kronig's model, as pointed out by Van Vleck,[10] yields vanishing transition probabilities even when pursued to second order in the orbit-lattice modulating interaction. The vanishing in first order is to be expected, but that in second order appears to be

due to a cancellation which would not occur if the inherent quantum asymmetry between emission and absorption probabilities (see Secs. 4 and 5) were contained in the calculation. Van Vleck includes this by use of quantized normal modes for the cluster of H_2O molecules about the Ti^{++} ion, and he finds a non-vanishing result in second order (third order in reference 10, inasmuch as the zero-order functions used do not yet include the effect of the $\lambda L \cdot S$ coupling).

In the present problem, we have no knowledge of the normal modes of the liquid "lattice." In fact, the free radical ion presents several complications. The ion itself is not spherically symmetric. When such is the case, as pointed out by Mizushima and Koide[26] and suggested independently by H. Primakoff, the spin-orbit interaction is not simply proportional to $L \cdot S$. The Dirac equation, after elimination of the small component wave functions, yields two interaction terms[27] which may be included[28] in the spin-orbit interaction:

$$\mathcal{H}_{spin\text{-}orbit} = -\frac{h^2}{4m^2c^2}(grad V)\cdot grad$$

$$+\frac{h}{4m^2c^2}s\cdot[(grad V)\times p]; \quad (56)$$

the potential energy function for the electron is V, s is the electron spin, and p is its linear momentum operator. A proper accounting of spin-orbit effects would thus require use of (56) instead of $\lambda L \cdot S$.

A second complication is that, for the $ON(SO_3)_2^{--}$ ion in aqueous solution, we may justifiably think of two sources for the orbit-lattice interaction which modulates the Stark splitting for the odd electron. One source involves the internal vibrations of the ion itself which produce fluctuating local electric fields over the orbit of the electron, and the other is the solvent as its randomly moving water dipoles also produce fluctuating local fields over the electron orbit.

Whereas a theoretical investigation of the interaction (56) presents grave difficulties for a free radical ion about which we know so little concerning the odd electron wave function, experiment may be able to distinguish which source of the orbit-lattice interaction is dominant, *provided*, of course, that spin-orbit coupling is involved in determining the W_R value measured experimentally. In order to shed some light on this important question, we brush aside our ignorance of the quantum nature of the motions and suppose that, for some fortuitous reason, the spectrum of their vibrations influences the Raman processes for $ON(SO_3)_2^{--}$ approximately as it does for Ti^{++} in titanium alum. For the latter Van Vleck obtains about 10^9 sec⁻¹ as the reciprocal relaxation time (which is essentially our W_R)

[23] R. deL. Kronig, Physica 6, 33 (1936).
[24] I. Waller, Z. Physik 79, 370 (1932).
[25] C. Kittel, Phys. Rev. 76, 743 (1949).

[26] M. Mizushima and S. Koide, J. Chem. Phys. 20, 765 (1952).
[27] L. I. Schiff, *Quantum Mechanics* (McGraw-Hill Book Company, Inc., New York, 1949).
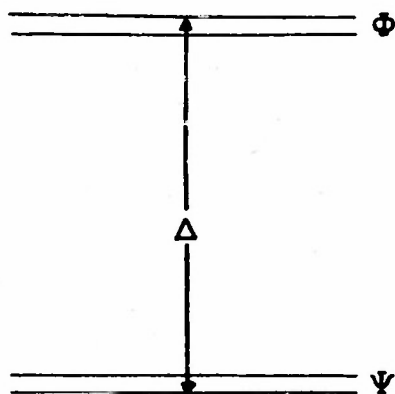[28] Reference 9, p. 130.

FIG. 6. The two lowest orbital levels.

due to Raman processes at normal temperatures and low fields. The matrix element in the transition probability is proportional to λ/Δ^3, where Van Vleck takes Δ, the Stark splitting, to be about 1000 cm^{-1} and λ/Δ to be about 1.5×10^{-1}. For free radicals, Δ may well be about the same as for titanium alum, but λ/Δ is much smaller; the spectroscopic splitting factor for $ON(SO_3)_2^{--}$ is 2.0055, measured in high fields,[29] indicating that $\lambda/\Delta \approx 10^{-3}$. Since W_R is proportional to the square of the matrix element, our utterly crude adjustment of the titanium result simply scales it down by the square of the ratio of the respective λ's, giving $W_R \sim 10^6$ sec^{-1}. In view of the high power of Δ involved and our wild approximations, this can hardly be called disagreement with the measured W_R, 2×10^6 sec^{-1}.

It is thus entirely possible that spin-orbit effects do lead to the observed W_R, and experiments are underway in this laboratory to examine whether it may be the solvent or the internal vibration of the ion which provides the orbit-lattice interaction.

14. RELAXATION THROUGH STATISTICAL PROCESSES OF SECOND ORDER

An interesting possibility for relaxation is brought out by our detailed expression (15) for the relaxation probability. In Van Vleck's calculation, discussed in the previous section, the quantity estimated corresponds only to U_{21}, and nothing has yet been said about the remaining function of U's in Eq. (15). Although this function may, as in Sec. 9, normally be small compared to U_{21}, such may not be the case if one must go to second or higher orders to obtain a nonvanishing U_{21}. Physically, this means that a relaxation mechanism which does not produce direct transitions between the levels under consideration may still effect relaxation by first carrying systems to a third level and then to the second. Such a process is second order in a *statistical* rather than a perturbation theory sense, i.e., energy is conserved for both transitions, whereas the second-order quantum perturbation transition probability does

[a] J. Townsend (unpublished).

not require energy conservation for the intermediate state.

The simple model of Kronig[24] is adequate for application of this idea to a free radical ion with spin-orbit coupling. We suppose that the odd electron of $ON(SO_3)_2^{--}$ is subject to a molecular Stark field which splits the orbital states into widely separated levels. For simplicity in illustrating the point, we follow Kronig by supposing that the two lowest orbital levels (see Fig. 6) are separated by energy Δ, whereas other orbital states have much higher energies and need not be considered further. Let these two orbital states, which retain their spin degeneracy, be ψ and ϕ. Then, if α and β refer to spin states $+\frac{1}{2}$ and $-\frac{1}{2}$, respectively, the effect of a spin-orbit interaction $\lambda \mathbf{L} \cdot \mathbf{S}$ is, to first order in λ/Δ, to produce the following mixtures of the unperturbed functions $\psi\alpha$, $\psi\beta$, $\phi\alpha$, and $\phi\beta$:

$$\Psi_1 = \psi\alpha - \frac{\lambda}{\Delta}b\phi\alpha - \frac{\lambda}{\Delta}a\phi\beta,$$

$$\Psi_2 = \psi\beta + \frac{\lambda}{\Delta}a^*\phi\alpha + \frac{\lambda}{\Delta}b\phi\beta,$$

$$\Psi_3 = \phi\alpha - \frac{\lambda}{\Delta}b\psi\alpha - \frac{\lambda}{\Delta}a\psi\beta, \qquad (57)$$

$$\Psi_4 = \phi\beta + \frac{\lambda}{\Delta}a^*\psi\alpha + \frac{\lambda}{\Delta}b\psi\beta.$$

Here,

$$a = \frac{1}{2}\int \phi(L_x + iL_y)\psi d\tau, \quad b = \frac{1}{2}\int \phi L_z \psi d\tau = -b^*. \quad (58)$$

In Eq. (58), ϕ is not denoted complex conjugate since, under the conditions of quenched orbital angular momentum, $\int \phi \mathbf{L} \phi d\tau = \int \psi \mathbf{L} \psi d\tau = 0$, it is possible to express ϕ and ψ as real numbers.[17]

If one sets up Eqs. (9) and (10) and solves for the saturation factor and for W_R associated with transitions between Ψ_1 and Ψ_2, he finds the following result:

$$W_R^{(12)} \cong \frac{1}{2}U_{14}. \qquad (59)$$

In obtaining Eq. (59), one uses $U_{12} = 0 = U_{34}$, as obtained from Eqs. (57). Also, in terms of absorption probabilities, the wave functions yield $U_{13}/U_{14} \approx U_{23}/U_{24} \approx (\lambda/\Delta)^2$. The relation (32) between absorption and emission holds, e.g.,

$$U_{41} = U_{14}e^{\Delta/kT}. \qquad (60)$$

Here, contrary to cases previously cited, the exponential factor is far from unity if Δ corresponds to about 1000 cm^{-1} ($\Delta/kT \sim 5$ at room temperature) and the result for W_R has been simplified by dropping absorption probabilities relative to emission probabilities.

We can evaluate U_{14} from Eq. (32) in which it must be recalled that we now require $j(\nu_{jk})$ at $\nu_{jk}=\Delta/h \approx 3\times10^{13}$ sec^{-1}. If we take $\tilde{F}_{op}(\mathbf{I},\mathbf{J})=1$ in Eq. (32) and denote

$$\langle(\langle 4|f(\mathbf{r})|1\rangle|^2\rangle_{Av}$$

$$=\left|\frac{\lambda}{\Delta}a\right|^2\left\langle\left|\int\psi f(\mathbf{r})\psi d\tau-\int\phi f(\mathbf{r})\phi d\tau\right|^2\right\rangle_{Av}$$

$$=\left|\frac{\lambda}{\Delta}a\right|^2\delta^2,\tag{61}$$

where δ^2 is a measure of the mean square of the electric interaction $f(\mathbf{r})$ which modulates the Stark effect, then, by Eq. (32),

$$U_{14}=h^{-2}|a|^2\left(\frac{\lambda}{\Delta}\delta\right)^2 j\left(\frac{\Delta}{h}\right).\tag{62}$$

Since $|a|^2\approx1$ and $j(\Delta/h)\approx1/(2\pi\Delta^2\tau_c/h^2)$ for $\Delta/h>1/\tau_c$, we have

$$W_R=\tfrac{1}{2}U_{14}\approx\left(\frac{\lambda}{\Delta}\right)^2\left(\frac{\delta}{\Delta}\right)^2\frac{1}{\tau_c}.\tag{63}$$

Taking $W_R=2\times10^6$ sec^{-1}, $\lambda/\Delta=10^{-2}$, and $\tau_c=10^{-11}$ for water solutions at room temperature, one finds that, if this mechanism is to be adequate, δ/Δ would have to be the order of unity. It is not unreasonable that the fluctuating Stark interaction arising from motions of the strong water dipoles or the internal vibrations of the ion might be comparable to the static Stark interaction, although the perturbation procedure would be somewhat strained in that event.

Again, the crudeness of our estimate does not lead us to very positive conclusions, but relaxation via the statistical second-order processes is not ruled out.

Whether quantum-mechanical or statistical second-order processes are involved in determining W_R, the experiments now in progress, which are aimed at distinguishing between the source of the modulating Stark field (internal vibrations in the ion or Brownian motions of the solvent), will serve a useful purpose.

15. SUMMARY

In water solutions of the free radical ion $ON(SO_3)_2^{--}$, width of the paramagnetic resonance seems to be determined by spin-lattice relaxation processes, at least for solutions sufficiently dilute to exhibit well-resolved hyperfine structure. The achievement of statistical equilibrium among the various hyperfine levels in low magnetic fields is more complex than in a simple two-level system. Where saturation methods are used, the *relaxation probability* is suggested as a more precisely defined quantity than the relaxation time.

At very low concentrations, the relaxation probability for the particular transition studied reaches a concentration-independent value of 2×10^6 sec^{-1}. Interaction between the free radical and nuclear dipoles of the solvent is demonstrated to be an inadequate mechanism both experimentally and theoretically. The interaction of the N^{14} quadrupole moment of $ON(SO_3)_2^{--}$ with the fluctuating electric field gradient due to the solvent is shown on the basis of an upper limit estimate to be an inadequate mechanism.

On the basis of very crude estimates, it is likely that spin-orbit coupling enables the spins to feel the effects of modulation of the Stark splitting which quenches electronic orbital angular momentum. However, it is not certain whether internal vibrations of the free radical ion or motions of the solvent molecules, or both, effect the modulation.

If the spin-orbit coupling is involved, an interesting possibility is that, for saturation experiments at least, *statistical* second-order processes in contrast to the quantum mechanical second-order processes of Van Vleck may be responsible for the observed relaxation.

Symmetry Classification of the Energy Levels of Some Triarylmethyl Free Radicals and Their Cations*

TING LI CHU AND S. I. WEISSMAN
Washington University, St. Louis, Missouri
(Received August 24, 1953)

The absorption and luminescence spectra of triphenylmethyl, tri-p-xenylmethyl, phenyl-di-p-xenylmethyl, diphenyl-p-xenylmethyl, and their cations have been determined. Polarization of the luminescence of each substance under excitation by plane polarized light has been examined. Assignment of symmetry classifications to the energy levels of these substances has been attempted.

IN this paper we describe our studies of the spectra of a set of triarylmethyl free radicals and their positive ions. The experiments consist of observations of the absorption spectra, the fluorescence spectra, and polarizations of the fluorescence spectra under excitation by polarized light. From a combination of these observations and some assumptions which appear to be not excessively bizarre, we have attempted to assign symmetry classifications to the electronic levels of the molecules under study. These molecules are triphenylmethyl, diphenyl-p-xenylmethyl, phenyl-di-p-xenylmethyl, tri-p-xenylmethyl, and their positive ions.

EXPERIMENTAL PROCEDURES

The free radicals were prepared by standard procedures.[1,2] Pure tri-p-xenylcarbinol was provided by Professor Lipkin. Diphenyl-p-xenylcarbinol and phenyl-di-p-xenylcarbinol were prepared by appropriate Grignard reactions. Their melting points were 135°C and 150–151°C (uncorrected), respectively, as compared with the accepted values of 136°C and 151°C. Triphenyl methyl was prepared from commercial triphenyl-chloromethane which had been purified by vacuum sublimation.

The solvent for the free radicals was a mixture of toluene and triethylamine containing 20 percent by volume of triethylamine. The absorption spectra were measured both at room temperature and liquid nitrogen temperature with a Beckman model D. U. spectropho-tometer.[3] The spectra at liquid nitrogen temperatures were checked by photography with an A.R.L. grating instrument. The fluorescence spectra were observed only from glassy rigid solutions at liquid nitrogen temperature. These were photographed with a Steinheil spectrograph.

The absorption and luminescence spectra of the free radicals are presented in Figs. 1–5, of the cations in Figs. 6–10.

Polarizations of the fluorescence were determined both by visual observation and by photography. The experimental arrangement, involving excitation in two almost contiguous strips by beams of equal intensity and mutually perpendicular polarization, has been described previously.[4]
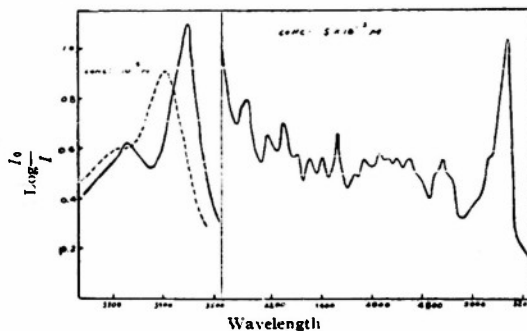

FIG. 1. Absorption spectrum of triphenylmethyl. Dashed curve at room temperature, solid curve at 77°K. One centimeter path length.

[1] Lewis, Lipkin, and Magel, J. Am. Chem. Soc. 66, 1579 (1947).
[2] T. L. Chu and S. I. Weissman, J. Am. Chem. Soc. 73, 4462 (1951).
[3] The free radicals were prepared under high vacuum. The absorption and fluorescence cells were in every case sealed off.
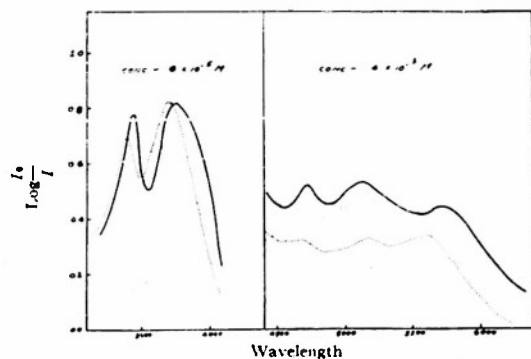[4] S. I. Weissman, J. Chem. Phys. 18, 1258 (1950).

Fig. 2. Absorption spectrum of diphenyl-p-xenylmethyl. Dashed curve at room temperature, solid curve at 77°K. One centimeter path length.
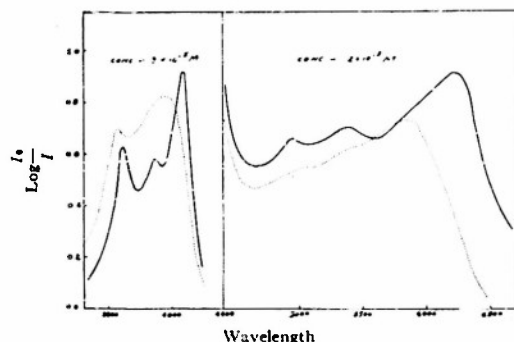

FIG. 3. Absorption spectrum of phenyl di-p-xenylmethyl. Dashed curve at room temperature, solid curve at 77°K. One centimeter path length.

The solvents employed for the cations were syrupy phosphoric acid (90 percent H_3PO_4) and phosphorus oxychloride. The carbinols were dissolved in the former, the chlorides in the latter. The phosphoric acid solutions form clear rigid glasses at low temperatures; these were used for observations of the luminescences of the cations. Phosphorus oxychloride is not suitable for use at low temperatures, but yields better transparency in the ultraviolet than phosphoric acid.

CLASSIFICATION OF LEVELS

Classification of the electronic levels requires knowledge of the symmetries of the equilibrium configurations of the molecules. In the absence of direct structure determinations we have assumed the following symmetries: for triphenylmethyl, tri-p-xenylmethyl and their cations C_3 (somewhat distorted from D_3h);[5] for the other molecules C_2 (distorted from C_{2v}). Let us consider first the molecules of trigonal symmetry. Both a simple

molecular orbital theory[6] and a valence bond treatment[7] lead to the assignment A_2'' (in symmetry D_3h) to the ground state of triphenylmethyl. We accept this assignment (A in symmetry C_3) and make further assignments on this basis. Should this assignment require correction, all the rest of our assignments may be corrected in a straightforward way.

In the absence of detailed calculations we assign the same classification (A_2'' in D_3h, A in C_3) to the normal state of tri-p-xenylmethyl.

The normal states of the cations, since these are even electron molecules, are in all likelihood totally symmetric.

Each free radical possesses a system of weak absorption bands in the visible,[8] and an intense absorption in the near ultraviolet. The strong absorptions we assign to allowed transitions. The only allowed transition from A_2'' consistent with the π electron hypothesis is to an E'' state. Hence we label the excited states responsible
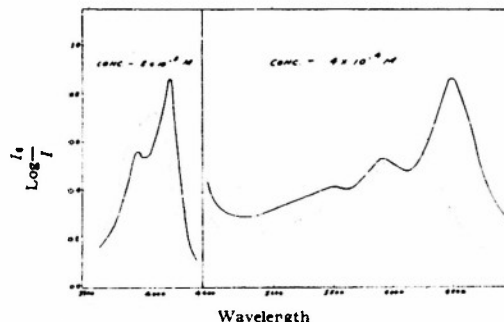

FIG. 4. Absorption spectrum of tri-p-xenylmethyl. Dashed curve at room temperature, solid curve at 77°K. One centimeter path length.
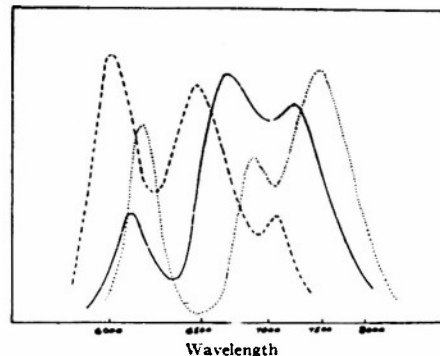

FIG. 5. Densitometer tracings of luminescence of free radicals. ·····tri-p-xenylmethyl; ——— phenyl-di-p-xenyl methyl; – – – – diphenyl-p-xenyl methyl. (Our curve for triphenylmethyl is indistinguishable from the one given by Lewis, Lipkin, and Magel.)

---

[5] We have not taken into account the distortion through the Jahn-Teller effect of these molecules from C_3 in some of their excited states. We have chosen the symmetry C_3 rather than D_3, because the latter does not permit mixing of s orbitals with p orbitals. The results of paramagnetic resonance studies of triphenylmethyl require such mixing.

[6] E. Huckel, Z. Physik. 83, 632 (1933).
[7] L. Pauling and G. W. Wheland, J. Chem. Phys. 1, 362 (1933).
[8] The approximate oscillator strengths are: tri-p-xenylmethyl, 0.02 phenyl-di-p-xenylmethyl 0.014; diphenyl-p-xenylmethyl 0.005. The value for triphenylmethyl is uncertain, because of strong association, but it is in the same range as the others.

for the strong near ultraviolet absorption in triphenyl-methyl and tri-p-xenylmethyl E' in symmetry D_3h, E in symmetry C_3.

Classification of the states responsible for the weak absorptions in the visible is facilitated by the polarization data. Lewis, Lipkin, and Magel[1] have observed that the triphenylmethyl fluorescence spectrum with its complex vibrational structure and the weak absorption are accurate mirror images of each other. The peak of shortest wavelength in fluorescence and the peak of longest wavelength absorption almost coincide. Hence the short wavelength fluorescence peak probably corresponds to a vibrationless transition. Its polarization is determined by the nature of the electronic states involved, while the polarization of the other peaks involves also the nature of the associated vibrational modes. When the fluorescence is excited by plane polarized light which is absorbed in the intense ultraviolet band, the "vibrationless" fluorescence peak is polarized at right angles to the polarization of the exciting light.[9] Since the intense absorption involves a transition with electric moment perpendicular to the trigonal axis of the molecule we conclude that the O–O
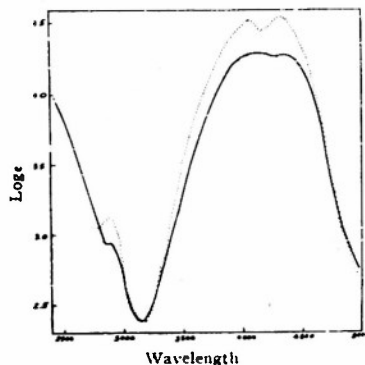

FIG. 6. Absorption spectrum at room temperature of triphenyl carbonium ion. Dashed curve in phosphoric acid, solid curve in phosphorus oxychloride.
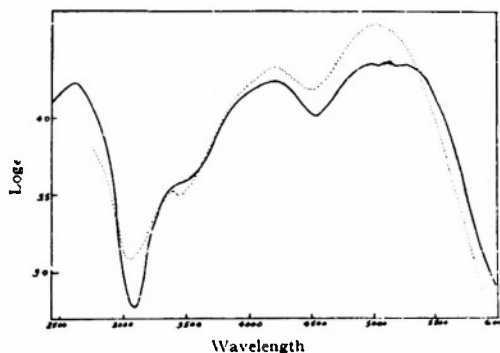

FIG. 7. Absorption spectrum of diphenyl p-xenyl carbonium ions at room temperature. Dashed curve in phosphoric acid, solid curve in phosphorus oxychloride.
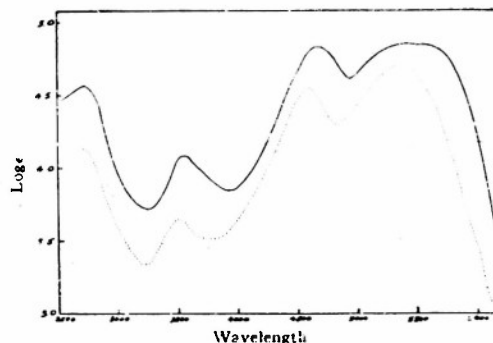
* The polarization ratio is approximately 0.9.

FIG. 8. Absorption spectrum at room temperature of phenyl-di-p-xenyl carbonium ion. Dashed curve in phosphoric acid, solid curve in phosphorus oxychloride.
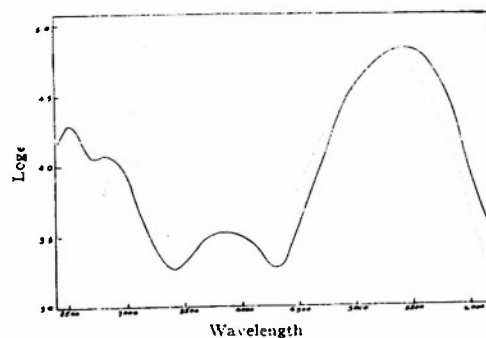

FIG. 9. Absorption spectrum at room temperature of tri-p-xenyl carbonium ion. Dashed curve in phosphoric acid, solid curve in phosphorus oxychloride.

transition occurs with electric moment parallel to the trigonal axis. Such a transition is forbidden (under the π-electron hypothesis) if the molecule possesses a reflection plane perpendicular to the trigonal axis. The O–O transition becomes partially allowed by distortion from the completely planar configuration. The propeller distortion or noncoplanarity of the four central carbon atoms or a combination of these effects is probably involved.

Because of incomplete resolution of the vibrational peaks reliable determination of the polarizations of the individual vibrational transitions is not possible. Nevertheless from the sign of the polarization at each maximum a guess as to the direction of the associated moment may be made. The signs of the polarizations and the guesses as to the nature of the various vibrations are given in Table I. These guesses are based on the assignment of classification A in $C_3(A_1''$ in $D_3h)$ to the excited electronic state. This assignment in turn is based on the polarization of the vibrationless transition.

For tri-p-xenylmethyl the situation is less clear cut. In the first place we note that the short wavelength fluorescence peak occurs at a considerably shorter wavelength—6200A—than the long wavelength absorption—6500A. Excitation at 6500A leads to no fluorescence. Certainly the fluorescent state and the state responsible
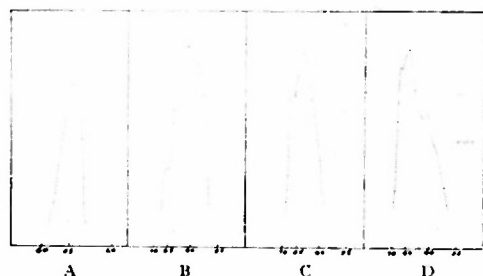
FIG. 10. Densitometer tracings of luminescence spectra of triphenyl carbonium ions. A. Triphenylmethyl carbonium. B. Diphenyl-p-xenyl carbonium. C. Phenyl-di-p-xenyl carbonium. D. Tri-p-xenyl carbonium.

for the absorption at 6500A are distinct. Our conclusions which are dependent on polarization of fluorescence apply to the fluorescent state.

The strong absorption near 4000A ($\epsilon \sim 4 \times 10^4$) we have associated with an allowed transition to an E'' state. The second peak at a frequency 1500 cm^{-1} higher than the main peak corresponds, we believe, to a transition to one of the vibrational levels of the E state rather than to another electronic state, or to absorption by an isomeric molecule. Excitation in each of the peaks separately yields the same fluorescence spectrum with the same polarization.

The fluorescence, when excited by plane polarized light of wavelength 4000A is positively polarized, with the polarization ratio between 1.2 and 1.3. Since a polarization ratio of 1.33 is anticipated for excitation by an $A_2'' \to E''$ transition with subsequent emission by an $E'' \to A_2''$ transition, we conclude that the weak transition occurs mainly through perturbation by assymetric vibrations of species e. Since the vibrational structure of the fluorescence is not nearly so well resolved as in the case of triphenylmethyl we are unable to make detailed assignments as we did in that case. It seems likely that in C_3 the symmetry of the excited electronic state is A and that e vibrations are responsible for most of the observed transition moment.

For both phenyl di-p-xenylmethyl and diphenyl-p-xenylmethyl, the strong ultraviolet absorption contains two well-separated peaks, which condition we believe

TABLE I. Classification of vibrational levels of triphenylmethyl from polarization of luminescence. Symmetry C_3 is assumed. V is the frequency of the peak in question, V_0 the frequency of the 0−0 peak.

$V_0 - V$ (cm^{-1})	Polarization	Species of associated vibration
0	negative	
230	positive	e
670	negative	a
970	uncertain	
1080	uncertain	
1550	negative	a
1850	positive	e
2210	negative	a
2510	negative	a

corresponds to the "splitting" of the doubly degenerate E state of the triphenylmethyl and tri-p-xenylmethyl under the lower symmetry. The behavior of diphenyl-p-xenylmethyl corresponds well to this supposition. Excitation in the peak at 3850 leads to fluorescence with strong positive polarization; excitation at 3400 leads to fluorescence of negative polarization. Hence absorption in the two bands must occur with transition moments perpendicular to each other. Further, the fluorescence, as in tri-p-xenylmethyl occurs with moment in the plane (since this moment is parallel to one of the "allowed" moments).

Similar behavior is exhibited by phenyl-di-p-xenylmethyl. The absorption in the visible is not forbidden in C_2v or C_2 symmetry. Excitation in the band at 4100A leads to strong positive polarization, at 3800 to weak positive polarization, and at 3600A to practically no polarization.[10] The first two peaks we ascribe to vibrational levels of a single electronic state, the third peak to another electronic state.

A summary of the positions of the electronic levels and the assignments is given in Table II.

TABLE II. Classification of the levels of the free radicals. Two classifications are given for each level. The first corresponds to the approximate symmetries D_3h or C_3v, the second in parentheses, to the symmetries C_2 or C_2.

Triphenyl-methyl	Tri-p-xenyl-methyl	Phenyl-di-p-xenylmethyl	Diphenyl-p-xenylmethyl
0 cm^{-1}: $A_2''(A)$	0 cm^{-1}: $A_1''(A)$	0 cm^{-1}: $B_1(B)$	0 cm^{-1}: $B_1(B)$
19 400 cm^{-1}: $A_1''(A)$	16 400 cm^{-1}: $A_1''(A)$	16 400 cm^{-1}: $A_2(A)$	16 700 cm^{-1}: $A_2(A)$
29 000 cm^{-1}: $E''(E)$	23 800 cm^{-1}: $E''(E)$	24 400 cm^{-1}: $A_2(A)$	26 700 cm^{-1}: $A_2(A)$
		27 800 cm^{-1}: $B_1(B)$	29 000 cm^{-1}: $B_1(B)$

THE CATIONS

The luminescence of the triphenylmethyl cation, since it seems to arise exclusively from a triplet state, was no help in classification of the singlet states of this ion. We shall not consider here the nature of this triplet state. Since the broad absorption with peak at 4000A is very intense, there is little doubt that the excited state is an E state. Similarly the strong absorption at 5200A in the tri-p-xenyl cation is ascribed to absorption to an E state. The fluorescence of this ion, because of its position, is ascribed to the reverse electronic transition of the absorption. For excitation by an $A_1 \to E$ transition followed by $E \to A_1$ luminescence a polarization ratio of 1.33 is expected. Positive polarization of about this magnitude was found when the luminescence was excited by light at 5500A. For both the phenyl-di-p-xenyl and diphenyl-p-xenyl cations the absorption in the visible is split into two bands, separated by about 4000 cm^{-1}. These bands we ascribe to transition to the two states into which the E state of triphenylmethyl or tri-p-xenyl cation splits under the lower symmetry. The polarization of luminescence of the phenyl-di-p-xenyl-

[10] In this case negative polarization is not achieved because of incomplete resolution of th bands.

methyl cations are in complete accord with this assignment. Excitation in the long wavelength absorption peak leads to a high positive polarization. The polarization ratio is about 2.5 as compared with the theoretical maximum of 3.0. Excitation in the next band leads to strong negative polarization of the luminescence. Thus the moments for the two transitions must be at right angles to each other.

The shorter wavelength absorption seems to differ considerably between the triphenylmethyl cation and the cations containing p-xenyl groups. All of the latter exhibit a strong absorption maximum ($\epsilon > 10^4$) in the neighborhood of 2800 angstroms, while the former is relatively transparent ($\epsilon < 10^3$) at this wavelength. A similar phenomenon occurs in the carbinols dissolved in non-ionizing solvents. At 2580 angstroms in methanol solution, triphenyl carbinol shows no absorption peak ($\epsilon = \sim 10^3$) while diphenyl-p-xenyl carbinol, phenyl-di-p-xenyl carbinol, and tri-p-xenyl carbinol each exhibit an absorption maximum with the extinction coefficients approximately in the ratio $1:2:3$. (The values are 2.4×10^4, 6×10^4, 9×10^4.) We suggest that absorption at 2800A in the cations as well as the absorption at 2580A in the carbinols is to be ascribed to a "localized" excitation in the p-xenyl group.[11]

---

[11] We use the term "localized excitation" to mean that the interaction between states in which the excitation energy is in a single p-xenyl group is not great enough to lead to an observable splitting. Thus for a molecule containing two p-xenyl groups, appropriate zero-order functions would be linear combinations of the functions which localize the excitation in single groups. If the energy difference between the state corresponding to these linear combinations is too small for observation, we speak of the excitation energy as "localized."

TABLE III. Classification of the levels of the cations. The classifications are given in symmetry D_3h for triphenyl carbonium and tri-p-xenyl carbonium ions; C_{2v} for diphenyl-p-xenyl carbonium and phenyl-di-p-xenyl carbonium ions.

Triphenyl carbonium	Tri-p-xenyl carbonium	Phenyl-di-p-xenyl carbonium	Diphenyl-p-xenyl carbonium
0 cm^{-1}: A_1'	0 cm^{-1}: A_1'	0 cm^{-1}: A_1	0 cm^{-1}: A_1
22 000 cm^{-1} E'	17 200 cm^{-1}: E'	17 200 cm^{-1} A_1	17 900 cm^{-1}: A_1
35 000 cm^{-1}: A_2'	25 600 cm^{-1}: A_2'	21 700 cm^{-1}: B_1	23 500 cm^{-1}: B_2
40 000 cm^{-1}?	36 000 cm^{-1}: E' and A_1'	28 200 cm^{-1}: A_1	37 000 cm^{-1}: A_1
		36 000 cm^{-1}: A_1 and B_2	

A consequence of this suggestion may easily be tested. For diphenyl-p-xenyl cations, the state in which excitation is localized in the single-p-xenyl is nondegenerate. Excitation by polarized light at 2800 angstroms should lead to a high positive polarization if emission from the fluorescent state occurs with a transition moment parallel to that of the absorption moment, to negative polarization if the moments are perpendicular. Measurement reveals a high positive polarization.

For phenyl-di-p-xenylmethyl cations, a much smaller degree of polarization is expected since excitation in the two p-xenyl groups may occur both with a moment parallel to the two fold axis and with a moment perpendicular to the axis. Under the assumption that excitation in the p-xenyl group occurs with moment along the long axis, we anticipate a polarization ratio of $13/11 = 1.2$. About 1.1 is observed, as contrasted to a ratio greater than 2 for the ions containing but one p-xenyl group.

If we accept the assumption that the absorption at 2800 angstroms in the p-xenyl group occurs with moment along the long axis, we are led to the assignments given in Table III.

Paramagnetic Resonance Spectra of Wurster's
Free Radical Ions*

S. I. WEISSMAN
Washington University, St. Louis, Missouri
(Received March 22, 1954)

THE complex hyperfine structure in the paramagnetic resonance spectrum of Wurster's blue free radical ion has been described in an earlier communication[1] from this laboratory. The spectra of a series of related free radicals have since been observed. Further, the spectrum of Wurster's blue ion, re-examined under higher sensitivity, has been found to contain thirty-nine lines disposed in thirteen triplets rather than thirty-three lines in eleven triplets as previously reported.

A description of the spectra of the free radicals (listed according to the names of the parent paraphenylenediamines) is given in Table I. The spectra of all the free radicals except the positive ion of NN dimethyl N'N' dideutero-p-phenylenediamine were observed from dilute solutions in ordinary water; the latter was dissolved in heavy water.

Unambiguous assignment of the origin of most of the splittings cannot yet be made. Comparison of the spectra of the NN dimethyl and NN dimethyl N'N' dideutero derivatives leads, however, to assignment of the 2.8-oersted interval in the former to interaction of the unpaired electron with the two amino protons. This splitting corresponds to a value of $|\psi|^2$, the square of the wave function of the unpaired electron, at each of these positions of 11.2×10^{22} cm^{-3} as compared with 2660×10^{22} cm^{-3} at the position of the proton in a 1s hydrogen atom. The 8.5-oersted interval in the dideutero compound may arise from interaction with the methyl protons. This assignment leads to a value 33×10^{22} cm^{-3} for $|\psi|^2$ at each of these positions. Summed over the six equivalent methyl protons, $|\psi|^2$ is about ten percent of the hydrogen 1s value. For the other compounds no assignments completely consistent with the observations have yet been devised. It is hoped that the investigations now being carried out in this laboratory of various isotopically substituted derivatives of these free radicals will lead to detailed interpretations of the splittings.

TABLE I. Spectra of positive ions of p-phenylenediaminal derivatives.

Derivative	Nature of spectrum
NNN'N' tetramethyl (Wurster's blue)	Thirteen triplets 7.4 oersteds between centers of triplets; 2.1 oersted between members of each triplet.
NN dimethyl (Wurster's red)	Twenty-seven almost equally spaced components. Interval 2.8 oersteds.
NN dimethyl-N'N' dideutero	Seven groups. Interval between groups 8.5 oersteds. Each group contains at least three components. Two more weaker groups may be present.
NN' dimethyl	Nine groups. Interval between groups 9.5 oersteds. Each group is complex, containing at least three components.
N methyl[a]	Twenty-four almost equally spaced lines. Interval about 2 oersteds.
Unsubstituted[a]	Fifteen lines; interval about 2 oersteds.

[a] Because of the instability of these free radicals their spectra were taken at sweep rates too rapid for trustworthy recording.

[1] Weissman, Townsend, Paul, and Pake, J. Chem. Phys. 21, 2227 (1953).

ELECTRON TRANSFER BETWEEN NAPHTHALENE NEGATIVE ION AND NAPHTHALENE[1]

Sir:

We have investigated the electron transfer reaction between naphthalene negative ion and naphthalene dissolved in tetrahydrofuran by a spectroscopic method.
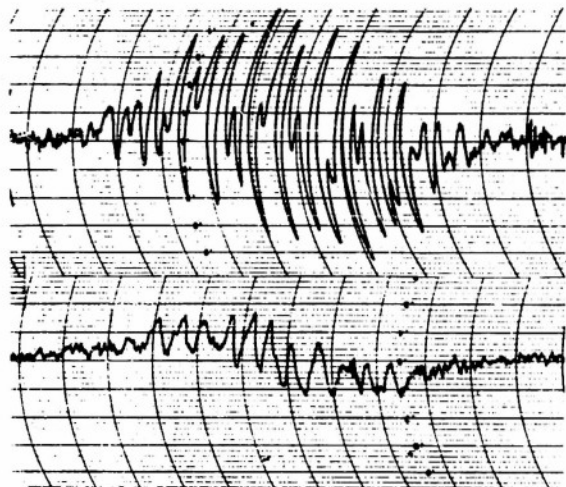
Naphthalene negative ion, in dilute solution in

Fig. 1.—First derivative with respect to magnetic field *versus* magnetic field of the paramagnetic resonance absorption of naphthalene negative ion: upper curve $(C_{10}H_8^-) = 5 \times 10^{-4} M$, $(C_{10}H_8) = 0.0$; lower curve $(C_{10}H_8^-) = 5 \times 10^{-4} M$, $(C_{10}H_8) = 0.35 M$.

tetrahydrofuran, possesses a complex paramagnetic resonance absorption spectrum of twenty-eight lines.[2] The lines are hyperfine components arising from interaction between the magnetic moment of the unpaired electron and the magnetic moments of the protons in the naphthalene negative ion.

For our purposes it is convenient to describe the spectrum by means of the reciprocal line breadths and reciprocal intervals. The reciprocal breadth of the individual lines, in dilute solutions of the sodium salt of naphthalene negative ion, is 6×10^{-7} sec-

onds; the reciprocal intervals are in the neighborhood of 3×10^{-7} seconds.

When naphthalene is added to a dilute solution of naphthalene negative ion, the paramagnetic resonance spectrum of the latter is altered. Addition of a small amount of naphthalene leads to broadening of the individual hyperfine components. As larger amounts of naphthalene are added the hyperfine components merge into a single peak with broad tails extending beyond the region encompassed by the original hyperfine pattern.

A representative pair of spectra taken at 30°, one with the naphthalene negative ion at a concentration of $5 \times 10^{-4} M$ and with no added naphthalene, the other with naphthalene negative ion at $5 \times 10^{-4} M$ and naphthalene at 0.35 M are given in Fig. 1. (The spectra are displayed as first derivative of absorption with respect to magnetic field versus field.) The broadening of the individual lines may be observed by direct measurement, by the merging together of close components, and by the decrease in amplitude between maxima and minima.[3]

The line broadening in the presence of naphthalene we ascribe to the transfer of electrons from naphthalene negative ions to naphthalene molecules. Such transfer limits the lifetimes of the quantum states responsible for the hyperfine pattern and consequently broadens the lines. According to this interpretation of the line broadening the mean lifetime of an individual naphthalene negative ion in the presence of 0.8 M naphthalene is 1.2×10^{-6} second. Under the assumption that the electron transfer follows a second order rate law, the rate constant at 30° is 1.0×10^6 liter mole^{-1} sec.$^{-1}$.

The method here described does not depend, as do most rate determinations, on some method of distinguishing reactants from products. The observations reveal directly the quantity of interest—the mean time during which a particular configuration persists undisturbed.

DEPARTMENT OF CHEMISTRY
WASHINGTON UNIVERSITY   R. L. WARD
ST. LOUIS, MISSOURI   S. I. WEISSMAN

(1) This research was supported by the United States Air Force, through the Office of Scientific Research of the Air Research and Development Command, and by the joint program of the U. S. Office of Naval Research and U. S. Atomic Energy Commission.

(2) D. Lipkin, D. E. Paul, J. Townsend and S. I. Weissman, *Science*, **117**, 534–535 (1953); S. I. Weissman, J. Townsend, D. E. Paul and G. E. Pake, *J. Chem. Phys.*, **21**, 2227 (1953); D. E. Paul, Ph.D. Thesis, Washington University, 1954.

(3) Under the conditions prevailing in this experiment the amplitude is proportional to the square of the reciprocal line breadth.

A Study of Manganous Complexes by Paramagnetic Resonance Absorption

THE paramagnetic resonance absorption of unstable metal complexes in aqueous solution has been explored and has been applied to the measurement of dissociation constants of such complexes. The method has the obvious limitation, in common with other magnetic methods, that direct measurements are confined to those ions and molecules which are paramagnetic. On the other hand, the method, in common with other spectroscopic methods, has the advantage that it can measure directly and rapidly the concentration of the free metal ion in solution without disturbing any pre-existing equilibrium state.

Manganous ion in dilute solid or liquid solution exhibits a hyperfine structure in its absorption when investigated by the paramagnetic resonance absorption method[1]. The existence of this hyperfine structure with its sensitive dependence on the chemical environment of the manganous ion and on type of bond in the molecule, coupled with the widespread biochemical activity of manganous ion, led us to initiate our studies with this ion.

The apparatus used in these studies records the derivative of the absorption curve with respect to magnetic field as a function of the field. Fig. 1 shows
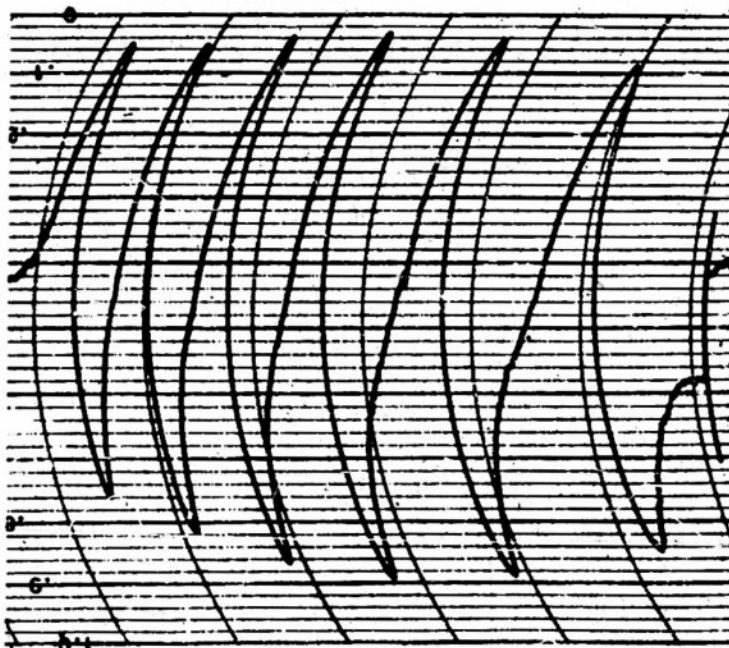

Fig. 1. Record of the derivative of the paramagnetic resonance absorption versus magnetic field of an aqueous solution of manganous chloride (0·005 M)

a typical record of the spectrum of an aqueous solution of manganous chloride ($0 \cdot 005\ M$), which was scanned from approximately 2,950 to 3,450 gauss in 5 min. with a modulation of 4 gauss and a microwave frequency of 9,000 Mc./s. Similar spectra can be obtained at concentrations ranging from $0 \cdot 001\ M$ to $0 \cdot 5\ M$ with approximately $0 \cdot 1$ ml. solution. The height of the derivative curve from the maximum to the minimum was found to be a linear function of the concentration of manganous ion in the range investigated, namely, $0 \cdot 001$–$0 \cdot 01\ M$, and it was therefore unnecessary to integrate the curves to obtain the concentration.

The phenomenon which made it possible to calculate dissociation constants was the disappearance of the hyperfine spectrum when the manganese formed a complex; the height of the peaks corresponded to the concentration of free manganous ion. When an equimolar concentration of ethylenediamine tetraacetic acid was added to a manganous chloride solution at pH $7 \cdot 5$, the peaks disappeared completely. A group of phosphate esters was investigated and it was found, for example, that with a series of increasing concentrations of glucose-6-phosphate, progressively smaller peaks were obtained corresponding to progressively lower concentrations of free manganous ion, as shown in Table 1. From these results, a dissociation constant $4 \cdot 76 \times 10^{-3}\ M$/litre for a complex of one manganese ion with one divalent glucose-6-phosphate ion can be calculated. The dissociation constant for glucose-1-phosphate was found to be $5 \cdot 18 \pm 0 \cdot 10 \times 10^{-3}$, and those of other monophosphate compounds were of the same order. The dissociation constants for adenosine diphosphate and triphosphate at pH $7 \cdot 5$ were too small to be measured because of the limited sensitivity of the apparatus now available. When $0 \cdot 001\ M$ adenosine diphosphate or triphosphate is added to $0 \cdot 001\ M$ man-

Table 1. DISSOCIATION CONSTANT OF THE MANGANESE GLUCOSE-6-PHOSPHATE COMPLEX

Initial concentration, $MnCl_2$ $0 \cdot 005\ M$ (tris-(hydroxymethyl)-aminomethane buffer, $0 \cdot 05\ M$), pH $= 7 \cdot 48$, $T = 33°$ C.

$$K = \frac{(Mn^{2+})\,(G\text{-}6\text{-}OPO_3{}^{2-})}{(Mn\ G\text{-}6\text{-}OPO_3)}$$

Initial concentration glucose-6-phosphate (M/lit.)	Final concentration Mn^{2+} (M/lit.)	$K \times 10^3$ (M/lit.)
$0 \cdot 0057$	$0 \cdot 00295$	$4 \cdot 90$
$0 \cdot 0114$	$0 \cdot 00187$	$4 \cdot 66$
$0 \cdot 0171$	$0 \cdot 00138$	$4 \cdot 95$
$0 \cdot 0228$	$0 \cdot 00100$	$4 \cdot 52$
		Average : $4 \cdot 76 \pm 0 \cdot 17$

Table 2. DISSOCIATION CONSTANTS OF MANGANESE COMPLEXES
Tris-(hydroxymethyl)-aminomethane buffer, 0·05 M, pH 7·5, T =
33° C.

Complexing agent	K (M/lit.)
Malonic acid	$2·20 \pm 0·26 \times 10^{-2}$
Glycylglycine	$1·45 \pm 0·10 \times 10^{-2}$
Histidine	$1·76 \pm 0·16 \times 10^{-2}$

ganous chloride at pH 7·5, the hyperfine structure
corresponding to the free manganous ion can no
longer be observed. This result sets an upper limit
on the dissociation constants for these compounds
of 2×10^{-5} M/litre.

Several other types of complexes were investigated
and the dissociation constants are summarized in
Table 2. The values for malonic acid and glycyl-
glycine agree in order of magnitude with those de-
termined by other methods (ref. 2) : differences in
temperature and concentrations may account for
the observed differences. However, the dissociation
constant for the complex with the imidazole group
of histidine is approximately one hundred times
larger than the value obtained by titration (ref. 3).
It may be that the assumptions involved in the
titration method are not correct for a compound
with three ionizing groups ; the shift observed in
pH may be due to the effect on the acid strength of
the amino-group in the manganese complex formed
between the carboxyl group and the imidazole group,
rather than to complex formation itself. It should
be pointed out that the temperature was not con-
trolled in these experiments, and the temperature in
the cavity was about 33° C.

The disappearance of the hyperfine structure in
the complexes studied gives some insight into the
type of bond. The explanation of the hyperfine
splitting due to manganous ion in solution, that is,
of the isotropic component of the hyperfine splitting,
as given by Abragam and Pryce[4], is the admixture
of the electronic configuration $(3s)^1 (3p)^6 (3d)^5 (4s)^1$
with the usual $(3s)^2 (3p)^6 (3d)^5$. If the 4s orbital
of manganous ion is occupied by electrons donated
by other atoms in the complex, as it would be for
any type of covalent bond formation, there could be
no admixture of 4s and therefore no hyperfine
structure. Changes in values of static magnetic
susceptibility are limited to complexes in which the
number of unpaired 3d electrons has changed ; thus,
in manganous compounds a change in static magnetic
susceptibility can be observed only when octahedral
complexes with d^2sp^3 covalent bonds are formed. On

the other hand, all possible types of covalent bond involve the $4s$ orbital and would lead to the disappearance of the hyperfine structure of the paramagnetic resonance absorption in solution. It may be that the presence or absence of the hyperfine structure will prove to be a more discriminating criterion of type of bond, ionic or covalent, than the usual magnetic criterion.

We have failed to detect the paramagnetic resonance spectrum of any complex. There should be a single peak characteristic of the unfilled $3d$ shell of the manganese in the complex even though the hyperfine structure disappears. Inability to detect such a peak is probably due to the lack of sensitivity of the apparatus for very broad peaks; at maximum modulation amplitude, the sensitivity is inversely proportional to the square of the width of the absorption peaks. It is hoped that improvements in instrumentation will permit extension of the method to a kinetic study of complex formation, in particular of metal–enzyme–substrate complexes, and also to the determination of dissociation constants of highly stable complexes.

MILDRED COHN
Department of Biological Chemistry,
    School of Medicine.

JONATHAN TOWNSEND
    Department of Physics,
    Washington University,
    St. Louis, Missouri.

[1] Bleaney, B., and Stevens, J. W. H., "Reports on Progress in Physics", 16, 108 (1953).
[2] Martell, A. E., and Calvin, M., "Chemistry of the Metal Chelate Compounds", 514 (New York, 1952).
[3] Kroll, H., J. Amer. Chem. Soc., 74, 2034 (1952).
[4] Abragam, A., and Pryce, M. H. L., Proc. Roy. Soc., A, 205, 135 (1951).

PARAMAGNETIC RESONANCE

TECHNICAL REPORT DISTRIBUTION LIST

August 10, 1953

PROFESSIONAL

Prof. Charles A. Whitmer
Department of Physics
Rutgers University
New Brunswick, New Jersey

Dr. Clyde A. Hutchison, Jr.
Department of Physics
University of Chicago
Chicago, Illinois

Prof. G. Pake and S. Weissman
Department of Physics
Washington University
St. Louis, Missouri

Dr. L. R. Maxwell
Naval Ordnance Laboratory
White Oak, Maryland

Dr. Charles Kittel
Department of Physics
University of California
Berkeley 4, California

Dr. Walter D. Knight, Jr.
Department of Physics
University of California
Berkeley 4, California

Dr. Bryce L. Crawford, Jr.
Department of Physics
University of Minnesota
Minneapolis, Minnesota

Professor C. P. Smyth
Department of Physics
Princeton University
Princeton, New Jersey

Dr. R. H. Dicke
Department of Physics
Princeton University
Princeton, New Jersey

Dr. P. Kusch
Head, Department of Physics
Columbia University
New York, New York

Dr. John W. Trischka
Department of Physics
Syracuse University
Syracuse 10, New York

Prof. W. A. Nierenberg
Department of Physics
University of California
Berkeley 4, California

Dr. Arthur Kip
Department of Physics
University of California
Berkeley 4, California

Prof. N. Bloembergen
Cruft Laboratory
Harvard University
Cambridge 38, Mass.

Prof. E. B. Wilson, Jr.
Department of Physics
Harvard University
Cambridge 38, Mass.

Dr. N. C. Baenziger
Department of Physics
State University of Iowa
Iowa City, Iowa

Dr. Immanuel Estermann
Code 419
Office of Naval Research
Washington 25, D. C.

Dr. H. C. Torrey
Department of Physics
Rutgers University
New Brunswick, New Jersey

Dr. F. Bloch
Department of Physics
Stanford University
Stanford, California

Dr. Walter Gordy
Department of Physics
Duke University
Durham, North Carolina

Dr. E. M. Purcell
Department of Physics
Harvard University
Cambridge, Mass.

Dr. R. H. Varian
Varian Associates
San Carlos, California

GOVERNMENTAL

1. Department of Defense

Research and Development Board
Information Office Library Branch
Pentagon Building
Washington 25, D. C. 2

Armed Service Technical Information
Agency
Documents Service Center
Knott Building
Dayton 2, Ohio 5

2. Department of the Navy

Chief, Bureau of Aeronautics
TD-4
Navy Department
Washington 25, D. C. 1

Chief, Bureau of Ordnance
Rea
Navy Department
Washington 25, D. C. 1

Chief, Bureau of Ships
Code 300
Navy Department
Washington 25, D. C. 1

Chief of Naval Research
Office of Naval Research
Washington 25, D. C.
Attn: Physics Branch (Code 421)...3

Director,
Naval Research Laboratory
Technical Information Officer
(Code 2000).....6
(Code 2021) 2
Washington 20, D. C.

Director,
Office of Naval Research Br. Office
150 Causeqay Street
Boston 14, Massachusetts.....1

Director,
Office of Naval Research Br. Office
346 Broadway
New York 13, New York.....1

Director,
Office of Naval Research Br. Office
86 East Randolph Street
Chicago 1, Illinois 1

Director,
Office of Naval Research Br. Office
100 Geary Street
San Francisco 9, Calif.....1

Director,
Office of Navl Research Br. Office
1031 East Green Street
Pasadena 1, Calif. 1

Officer in Charge
Office of Naval Research London
Branch Office
Navy #100
Fleet Post Office
New York, New York 2

Physics Department
Post Graduate School
U. S. Naval Academy
Annapolis, Maryland

U. S. Naval War College
Newport, Rhode, Island

Librarian
U.S. Navy Post Graduate School
Monterey, California

U. S. Naval Electronics Lab. Library
San Diego 52, California

Director,
Physics Research
Naval Ordnance Laboratory
White Oak, Maryland

Director
Physics Research
Naval Ordnance Test Station
Inyokern
China Lake, California

Mr. B. Allison Long, Jr.
Chief, BUAer (AER-EL-421)
Navy Department
Washington 25, D. C.

Mr. Perley G. Nutting
BUOrd (Re4e)
Room 4124, Main Navy Bldg.
Navy Department
Washington 25, D. C.

Mr. C. Scott Woodside
BUShips (Code 853)
Navy Department
Washington 25, D. C.

LCDR L. A. Franz
Electronics Division
ODCNO for Logistics
Room 4A-538, Pentagon
Washington 25, D. C.

Mr. Charles E. Keener
Control and Guidance Div., AEEL
U.S. Naval Air Development Center
Johnsville, Pennsylvania

Dr. John A. Sanderson
Naval Research Laboratory (Code 3700)
Washington 25, D. C.

3. Department of the Air Force

Commanding General
Air Research and Development Command
Attn: Office of Scientific Research
Post Office Box 1395
Baltimore 3, Maryland 2

Mr. Alva L. Brothers, Jr.
Wright Air Development
Center (WCEG)
Wright Patterson Air Force
Base, Ohio

Dr. Paul J. Ovreoo
WCERD-3, Weapons Components Div.
Wright Patterson Air Force
Base, Ohio

Mrs. Frank M. Field
Hqs. USAF, Electronics Div.
(AF/DRD-EL3)
Directorate of Research and
Development
Room 4C-331, Pentagon
Washington 25, D.C.

Mr. Joseph J. Knopow
Hqs. USAF Directorate of
Ordnance
Operations Analysis Div.,
AFOOP/OA
Room 5C-283, Pentagon
Washington 25, D. C.

Capt. Constantine A. Pappas
Air Research and Development
Command
(RDDRE) P. O. Box 1395
Baltimore 3, Maryland

Mr. James R. Rone
Armament Division (AFDRD)
Directorate of Research and
Development
Office, Deputy Chief of Staff,
Development
Hqs. USAF, Room 4C-349, Pentagon
Washington 25, D. C.

Dr. Walter Byers
Hqs., 1125th USAF Field Activities
Group (ATIAE-4)
Wright Patterson Air Force Base,
Ohio

Dr. Joseph P. Casey, Jr.
Physics Branch (CRRDP)
Air Force Cambridge Research
Center
230 Albany Street
Cambridge, Massachusetts

4. Department of the Army

Commanding Officer
Engineering Research and Development Laboratories
Fort Belvoir, Virginia
Attn; Technical Information
Intelligence Branch

Office of Ordnance Research
Box C.M., Duke Station
Durham, North Carolina 2

Signal Corps Engineering Lab.
Fort Monmouth, New Jersey
Attn: Technical Information Officer

Mr. George E. Brown
Engineer Research and Development Labs.
The Engineer Center
Fort Belvoir, Virginia

Mr. Harry Dauber
Applied Physics Branch
Evans Signal Laboratory
Belmar, New Jersey

Mr. Henry T. Gibbs
Electrical Branch, R. and D. Div.
Office, Chief of Engineers
Room 1038, T-7
Washington 25, D. C.

Commanding Officer
(FCIG) Box 7989
Frankford Arsenal
Philadelphia 1, Pennsylvania
Attn: Dr. M. L. E. Chwalow

Mr. John E. Darr, Jr.
ORDTR, D/A, Office Chief of Ordnance
Research and Development Div.
Artillery Branch
Room 2D-378, Pentagon
Washington 25, D. C.

Mr. Norman Stulman
Engrg. and Tech. Div., OCSigO
Special Projects Branch
Room 2B-269, Pentagon
Washington 25, D. C.

Office, Chief of Armu Field
Forces
Research and Development Sec.
Attn: Col. Frank F. Wilkins
Fort Monroe, Virginia

5. Department of Commerce

Director
National Bureau of Standards
Washington 25, D. C. 1

Director
National Bureau of Standards
Corona, California 1

6. Others

Dr. Richard C. Lord
Dept. of Chemistry
Mass. Inst. of Technology
Cambridge 39, Mass.

Dr. R. Bowling Barnes
Olympic Development Co.
30 Commerce Road
Stamford, Connecticut
Dr. George A. Morton
RCA Laboratories
Princeton, New Jersey

Mr. Fordyce Tuttle
Eastman Kodak Co.
Camera Works
333 State Street
Rochester 4, New York

Armed Services Technical Information Agency

AD

44486

UNCLASSIFIED